NuclearScience
Computing CenteratCCNU

QCD Chiral Crossover Line from Lee–Yang Edge Singularities

Heng-Tong Ding

Central China Normal University

HTD, S. Mukherjee, P. Petreczky, Kai-Fan Ye, arXiv:2608.05752

Kai-Fan Ye et al., [Bielefeld-BNL-CCNU], in preparation

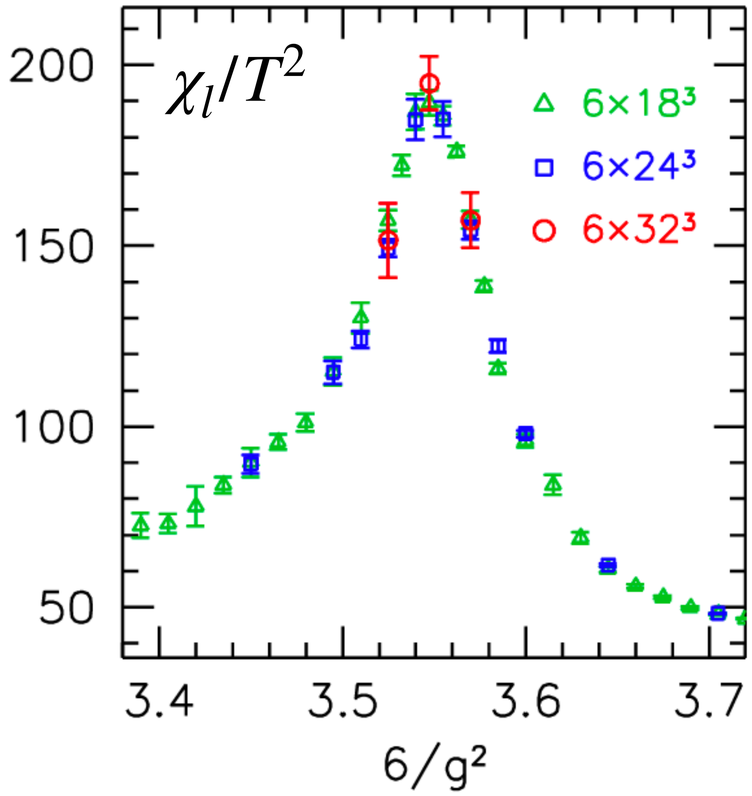
The 3rd international workshop on physics at high baryon density (PhD 2026)

Nov. 10-13, 2026@Dalian

QCD transition at μ_B=0 in Nature

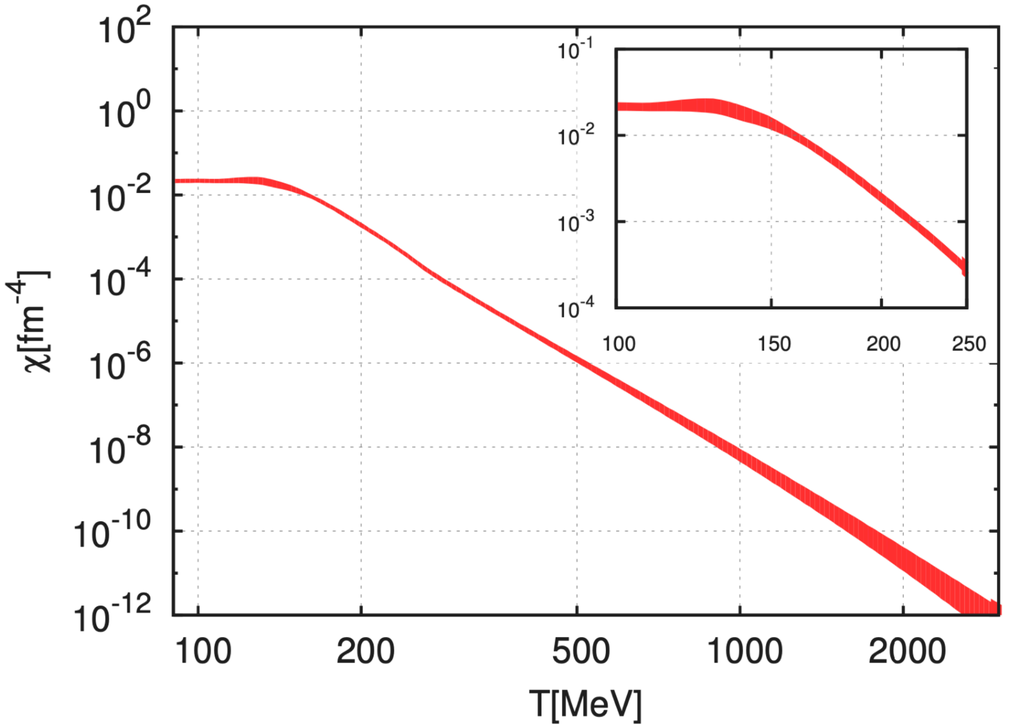
Not a true phase transition but a rapid crossover

chiral susceptibility



Y. Aoki et al., Nature 443 (2006) 675-678

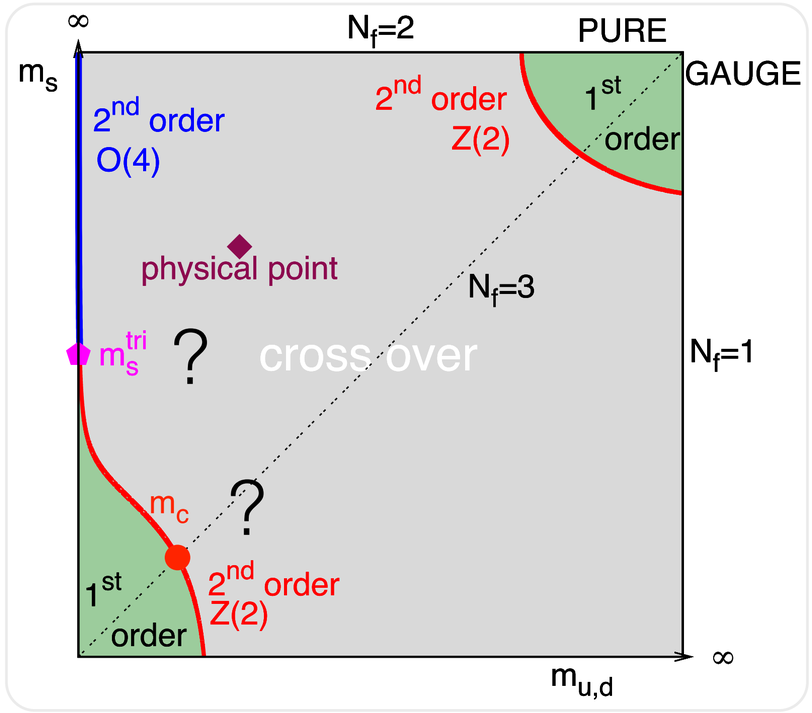
topological susceptibility



[Wuppertal-Budapest], arXiv:1606.07494, Nature 2016

QCD criticality relevant to the real world

Columbia plot:
QCD phase diagram in quark mass plane



- At physical point: crossover type transition

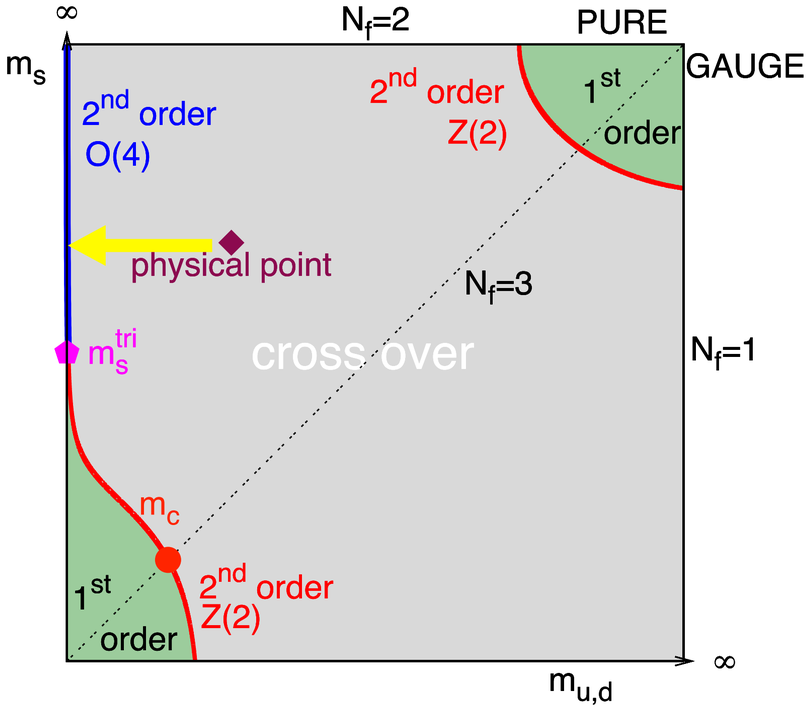
[HotQCD] PRL,113(2014)082001, PRD 85(2012)054503
[Wuppertal-Budapest], JHEP 1009 (2010) 073

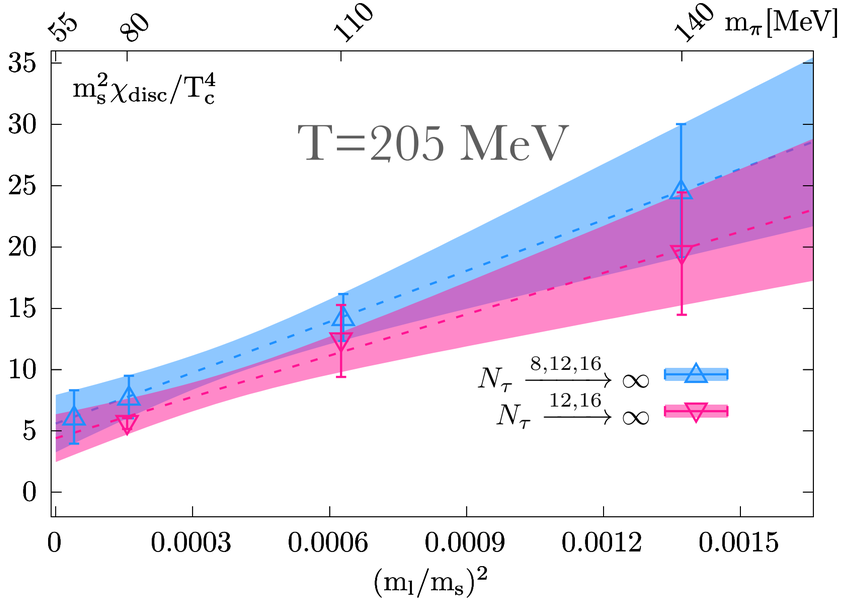
- Critical lines of second order transition
  - N_f=2: O(4) universality class — Pisarski & Wilczek PRD '84,Kogut & Sinclair, PRD '06 …
  - N_f=3: Ising universality class — Karsch, Laermann, Schmidt PLB '04,...

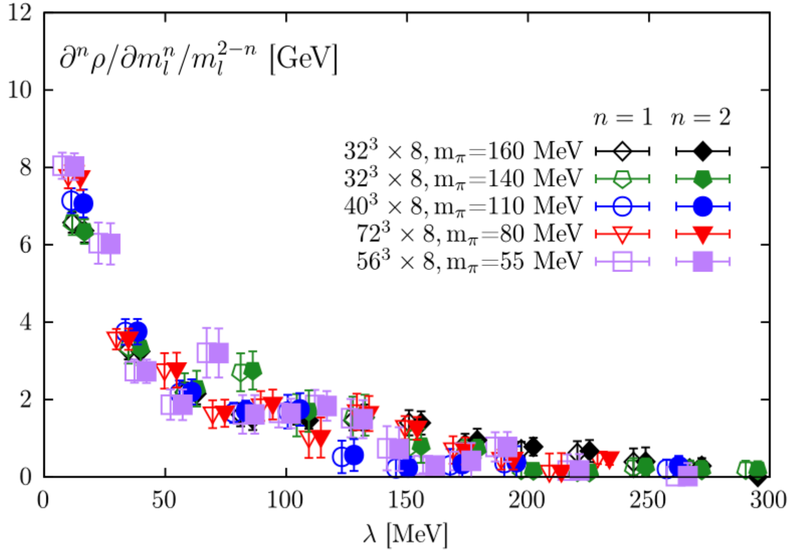
- N_f=2+1 QCD: fate of axial U(1) symmetry ? O(4) or 1st order ?
- Criticalities that are relevant to QCD thermodynamics at the physical point ?
- Fundamental scale of QCD: chiral T_c^0 ?

Which criticalities relevant to the chiral crossover

Indication from axial U1 anomaly







HTD et al., PRL 126 (2021) 082001

Relevant: 2nd order chiral phase transition belonging to O(4) universality class

as axial U(1) symmetry is manifested even at T =205 MeV ($\chi_{disc} \neq 0$)

See also the recent review on the axial U1 anomaly at finite T: HTD, arXiv:2609.21907

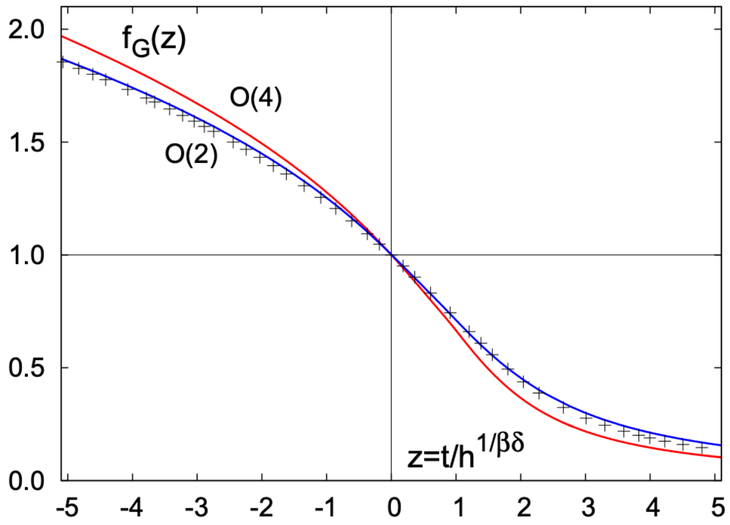
Chiral phase transition and universality class

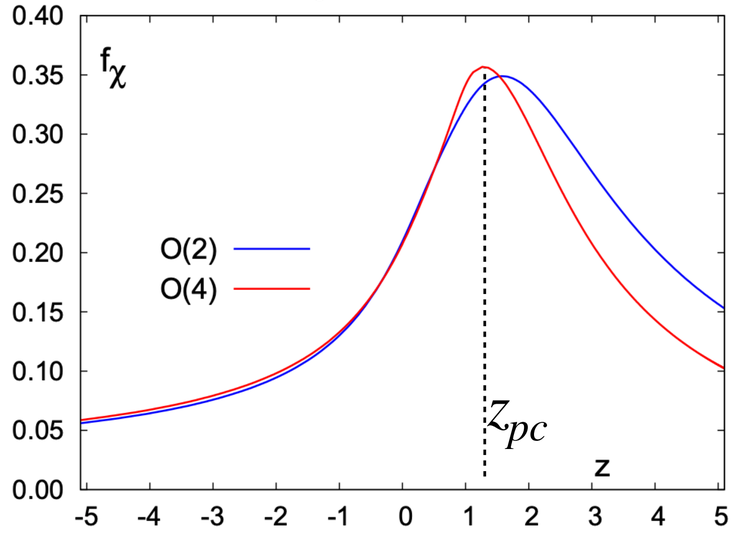
- Behavior of the free energy close to critical lines

$$f(m,T)=f_s(z)+f_{reg}\,, \qquad z=t/h^{1/\beta\delta}$$

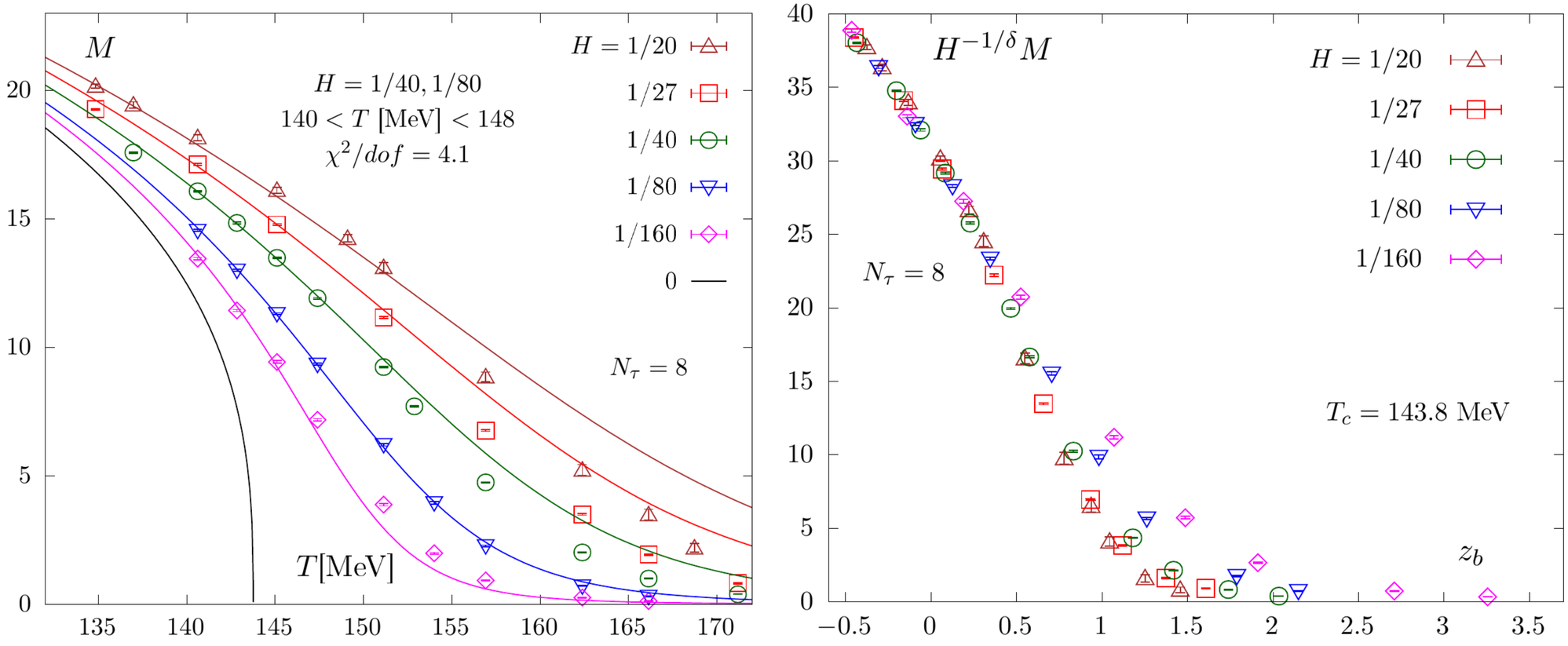
$$h=\frac{I}{h_0}\frac{m_l}{m_s} \qquad t=\frac{I}{t_0}\frac{T-T_c}{T_c}$$

- Universality scaling behavior of
  - Order parameter: $M=-\partial f_s(t,h)/\partial H = h^{1/\delta} f_G(z) + M_{reg}$
  - Order parameter susceptibility: $\chi_M=-\partial M/\partial H = \frac{1}{h_0} h^{1/\delta-1} f_\chi(z) + \chi_{M,reg}$





Chiral universality in lattice QCD



Different light-quark masses follow a common scaling curve

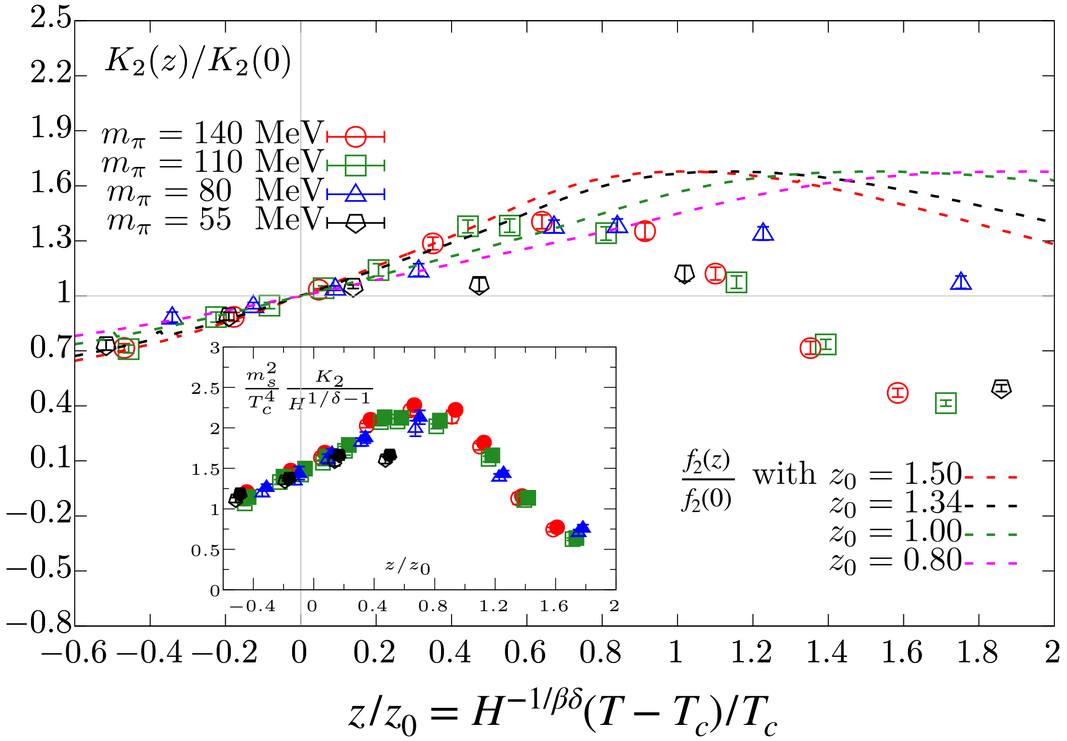
O(4) continuum expectation O(2) at finite staggered lattice spacing

HTD et al., PRD 109 (2024) 114516

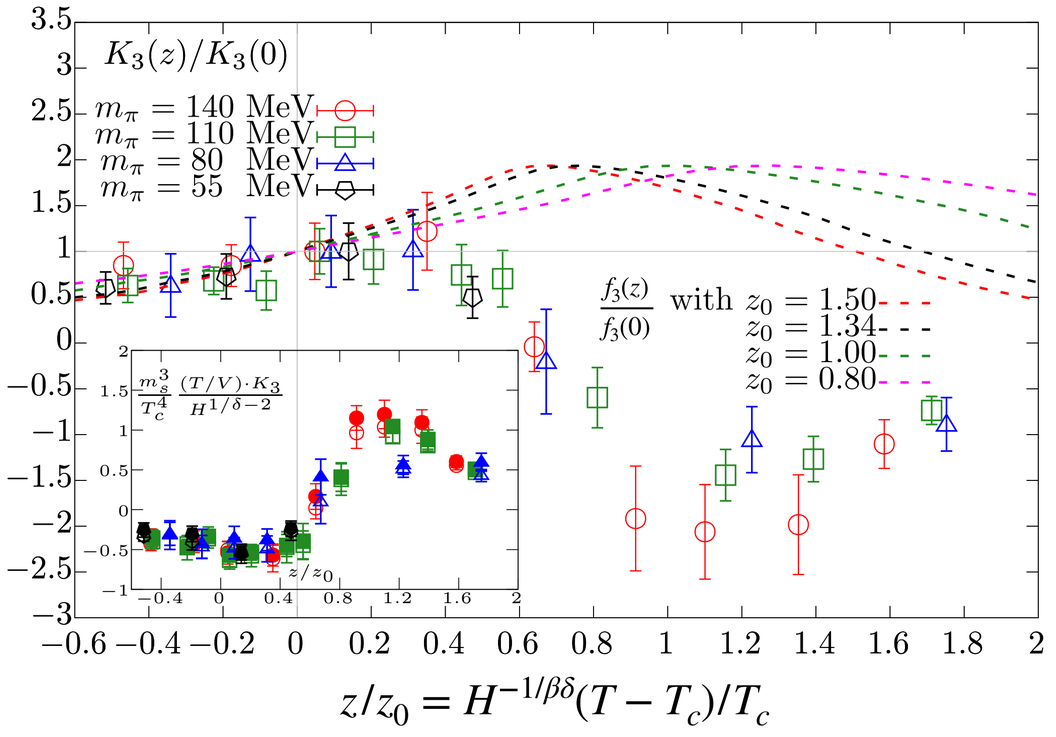
O(N) scaling behavior of $\mathbb{K}_n(\bar{\psi}\psi)$ at $\mu_B = 0$

HISQ, Nt=8, pion mass ranging from 140 to 55 MeV

$\mathbb{K}_2(z) \sim m_l^{1/\delta-1} f_2(z), \quad \mathbb{K}_2(z)/\mathbb{K}_2(z=0) \sim f_2(z)/f_2(0)$



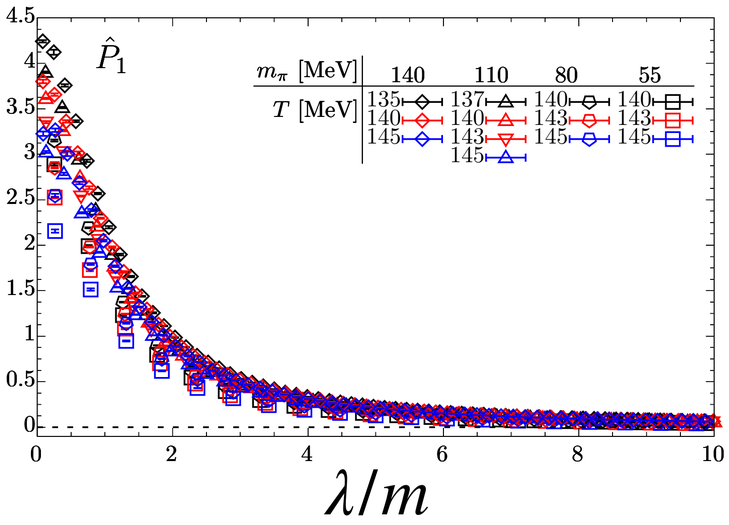
$\mathbb{K}_3(z) \sim m_l^{1/\delta-2} f_3(z), \quad \mathbb{K}_3(z)/\mathbb{K}_3(z=0) \sim f_3(z)/f_3(0)$

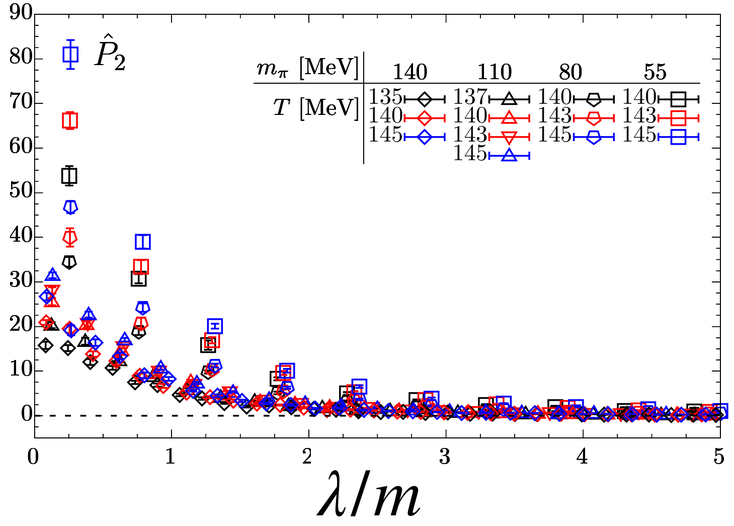


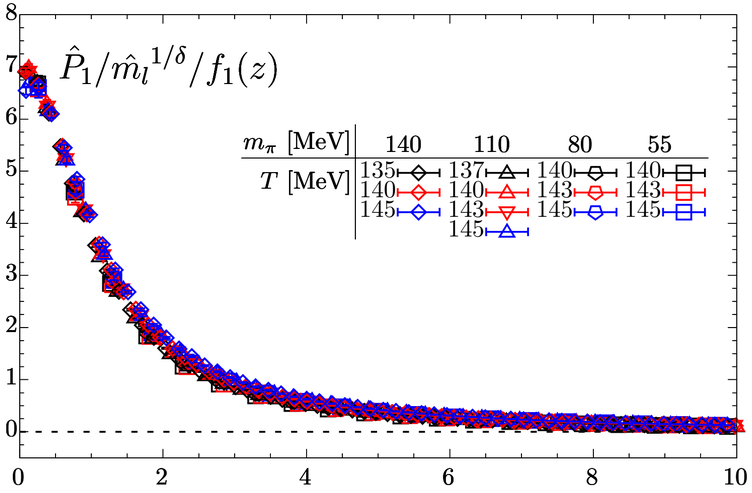
In the proximity of Tc: $\mathbb{K}_n(\bar{\psi}\psi) \sim m^{1/\delta-n+1} f_n(z)$!

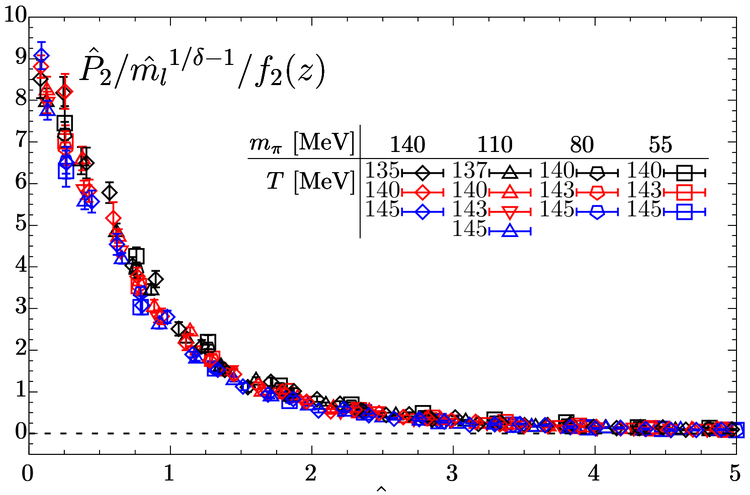
HTD, W.-P. Huang, S. Mukherjee and P. Petreczky, PRL 131(2023)161903

Microscopic encoding of Macroscopic criticality









N_τ=8 lattices

Marco: $\mathbb{K}_n(\bar{\psi}\psi) \sim m^{1/\delta-n+1} f_n(z)$

$$\mathbb{K}_n(\bar{\psi}\psi) = \int_0^\infty P_n(\lambda)\, \mathrm{d}\,\lambda$$

$$P_n(\lambda) = \int_0^\infty K_1[P_U(\lambda;m_l), P_U(\lambda_2;m_l), \cdots, P_U(\lambda_n;m_l)] \prod_{i=2}^{n} \mathrm{d}\lambda_i$$

Mirco: $P_n(\lambda) = m^{1/\delta-n+1} f_n(z)\ g(\lambda/m)$

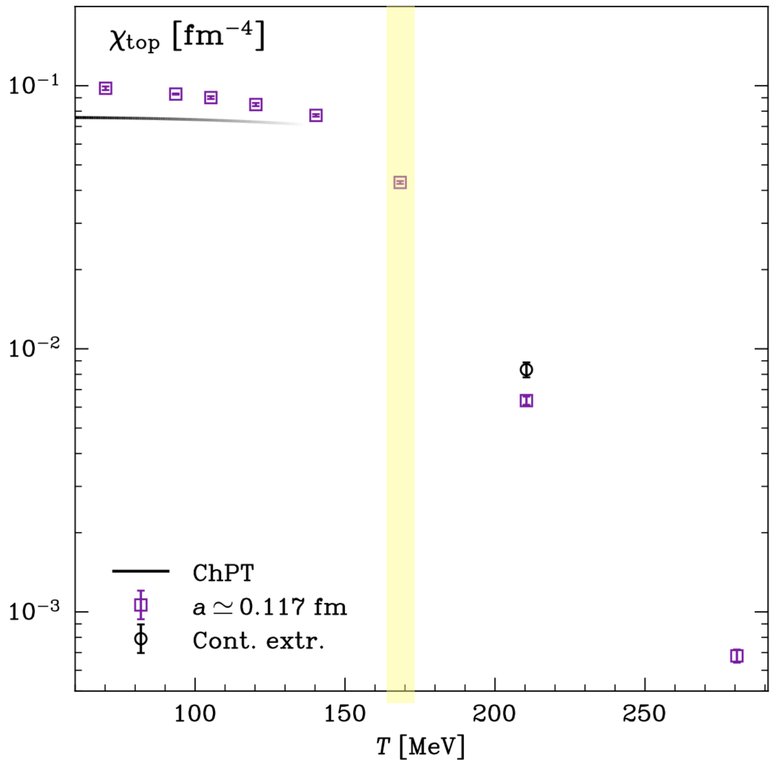
HTD, W.-P. Huang, S. Mukherjee and P. Petreczky, PRL 131(2023)161903

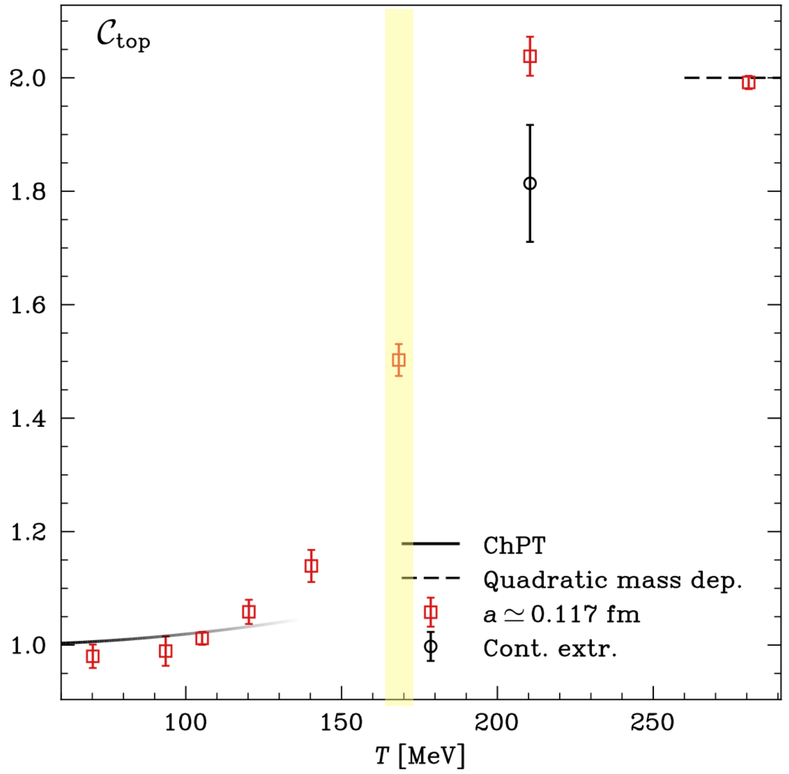
Chiral response of QCD topology across the thermal crossover

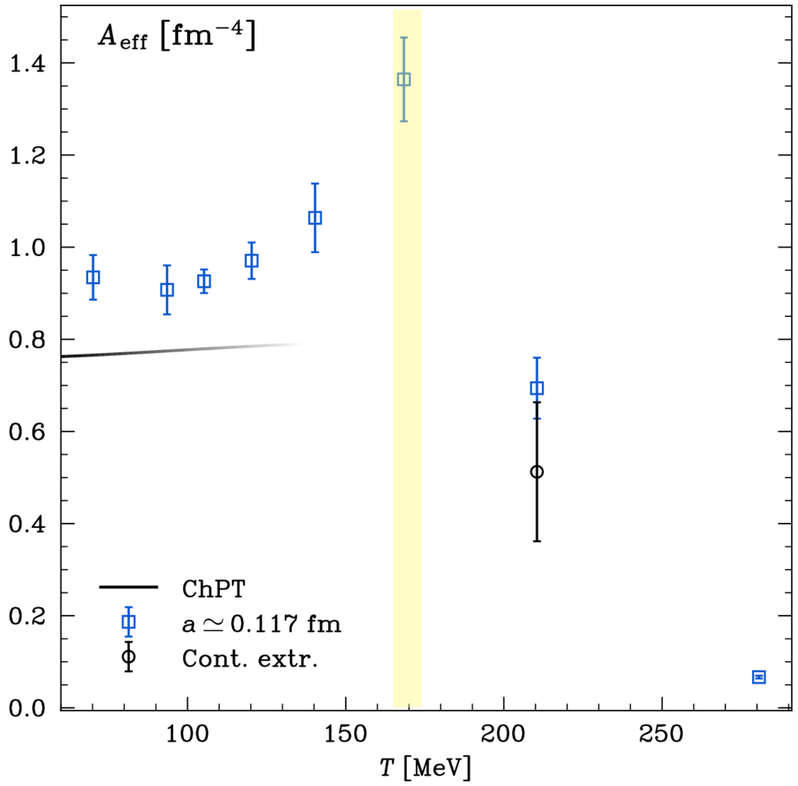
Topological susceptibility $\chi_{\rm top}$: suppression

$C_{top} = \partial \ln \chi_{top} / \partial \ln m_l$: increasing response

$A_{eff} = \chi_{top} H^{-C_{top}}$: a crossover peak



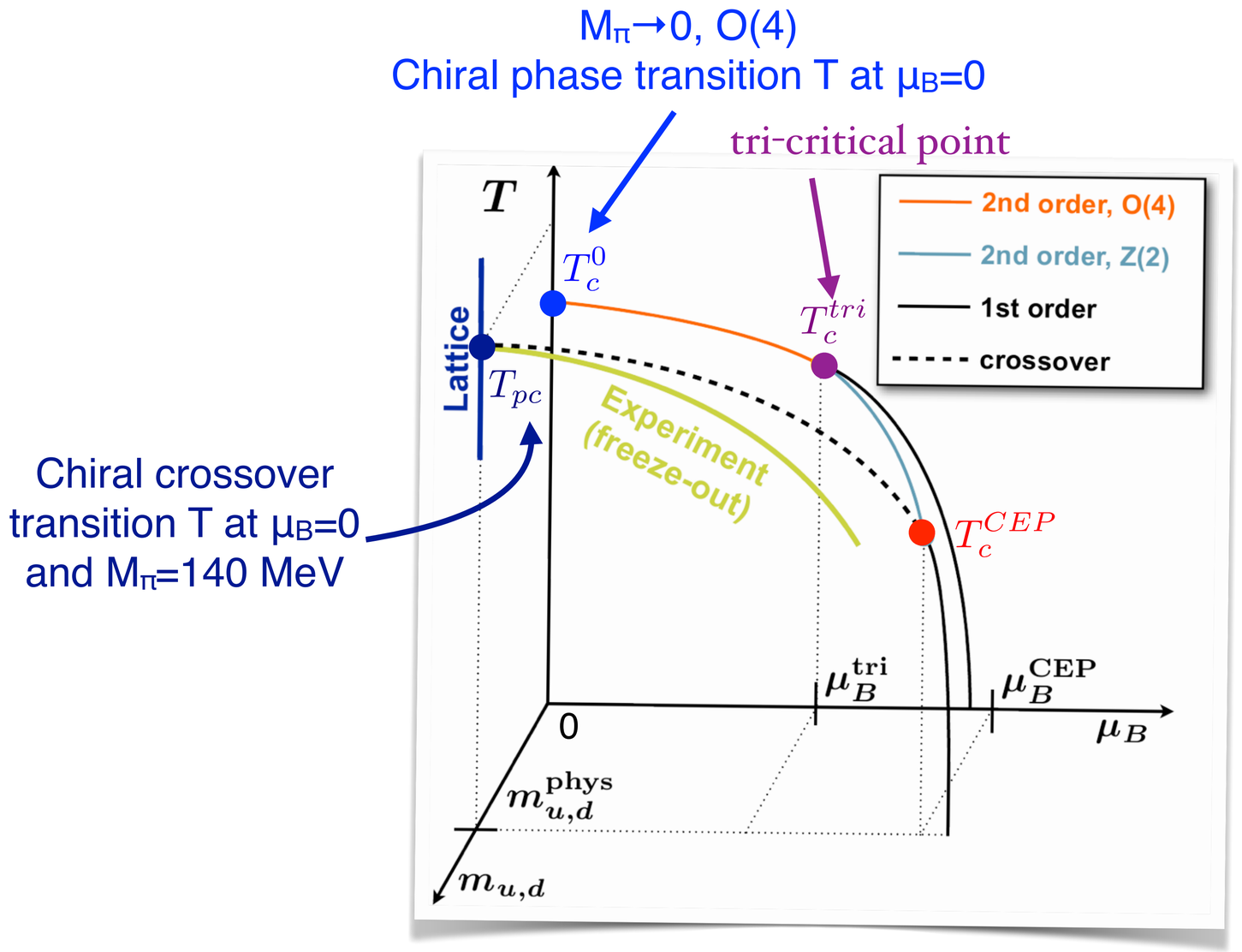




$T_{pc} \approx 170$ MeV for this lattice setup ($m_\pi = 220$ MeV)

HTD, J.-B. Gu, J. Hernández Hernández, S.-T. Li & J. Ni, arXiv:2611.09150

Upper bound for T_c^{CEP} at Critical End Point (CEP)



- $T_c^0(\mu_B)$ decreases as μ_B increases from LQCD

P. Hegde & HTD, PoS LATTICE2015 (2016) 141
O. Kaczmarek et al., PRD83 (2011) 014504

- Tri-critical mean-field:

$$T_c^{tri} - T_c^{CEP}(m_q) \propto m_q^{2/5}$$

M. A. Halasz et al., PRD 58 (1998) 096007
M. Buballa, S. Carignano, PLB791(2019)361
Y. Hatta & T. Ikeda, PRD67 (2003) 014028

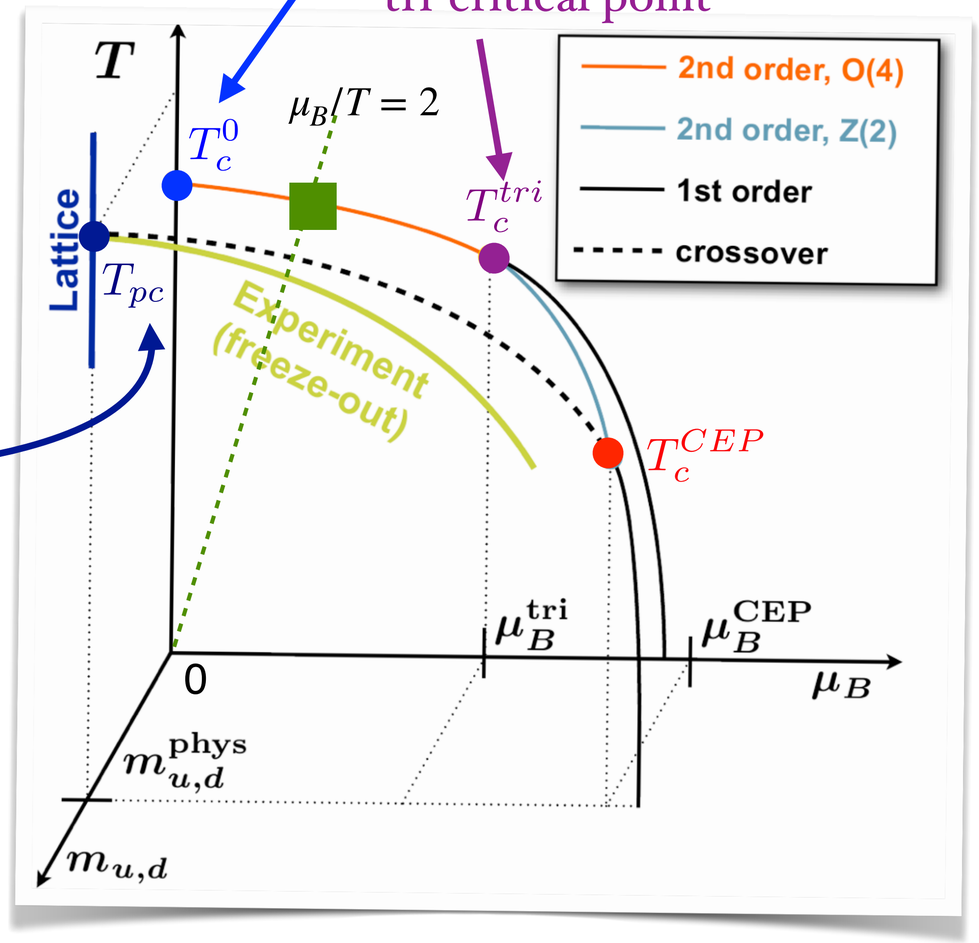
- Indications:

$$T_{pc}^{phys} > T_c^0 > T_c^{tri} > T_c^{CEP}$$

Upper bound for T_c^{CEP} at Critical End Point (CEP)

$M_\pi \to 0$, O(4)
Chiral phase transition T at $\mu_B=0$

Chiral crossover transition T at $\mu_B=0$ and M_π=140 MeV



- Continuum and chiral extrapolated

$$T_c^0(\mu_B = 0) = 132^{+3}_{-6}\ \text{MeV}$$

HTD et al.[HotQCD], PRL 123 (2019) 062002
See consistent results using Wilson fermions from Kotov et al., PLB 823 (2021) 136749

- Chiral curvature line on Nt=8 lattices

$$T_c^0(\mu_B) = (1 - 0.015(1)\ \hat{\mu}_B^2)\ T_c^0(0)$$

HTD et al.[HotQCD], PRD 109 (2024) 114516

- Updated upper bound with κ_2(Nt=8)

$$T_c^{CEP} \lesssim T_c^0(\hat{\mu}_B = 2) \sim 125\ \text{MeV}$$

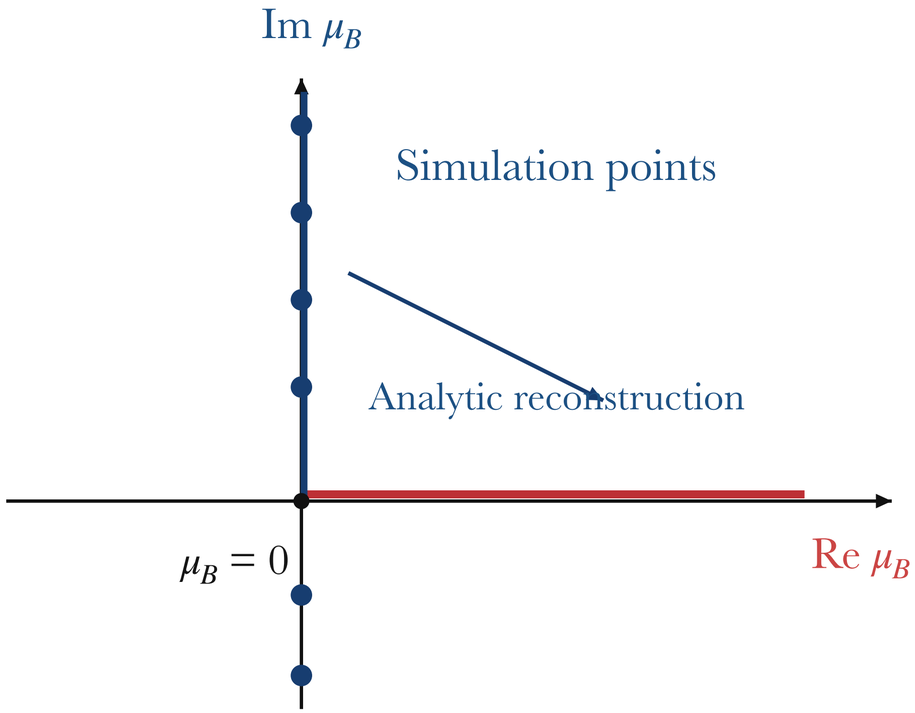
Imaginary μ_B opens a route to real QCD thermodynamics

Real μ_B: the sign problem

Complex determinant obstructs
standard importance sampling

Imaginary μ_B: simulations are possible

Combine imaginary-μ_B data
with derivatives at $\mu_B = 0$



Lee–Yang theory

Zeros pinch the real axis as V → ∞ → a phase transition

Nearby off-axis zeros → rapid but smooth crossover

How can the partition function vanish?

Ding et al., arXiv:2608.05752. Adam et al., arXiv:2507.13254. Lee & Yang (1952).

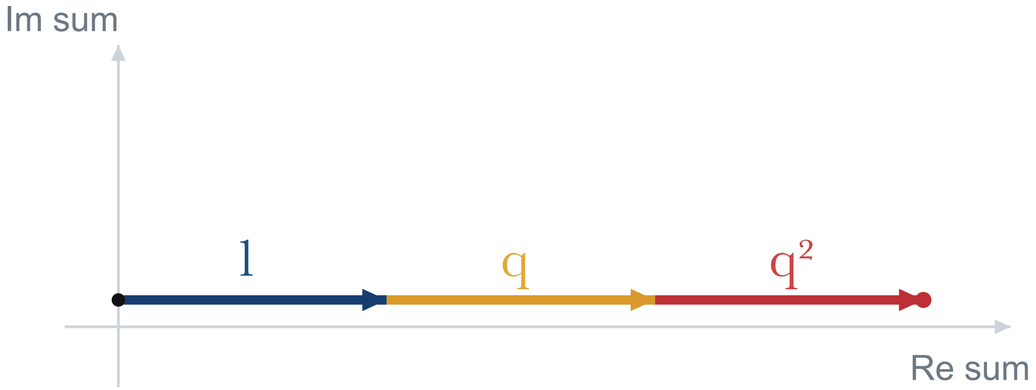
Lee–Yang zeros: how complex weights cancel

Three equal-energy states with particle numbers N=0,1,2

$$Z(q) = 1 + q + q^2$$

q is the fugacity: $q = \exp(\mu/T)$

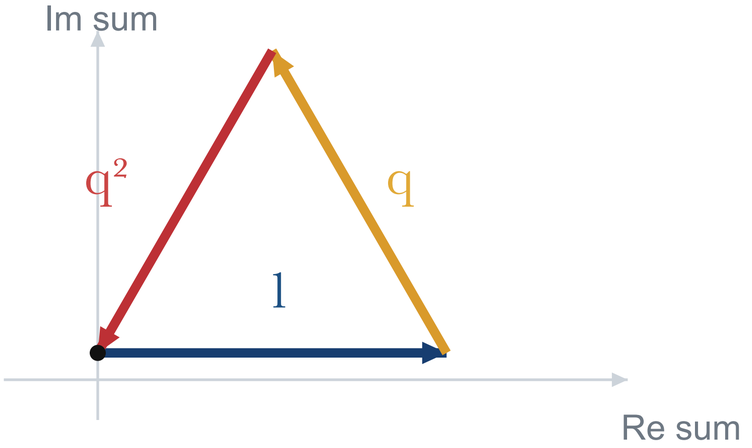
Real fugacity: $q = 1$



$Z = 3$

The terms add

Complex fugacity: $q = \exp(2\pi i/3)$



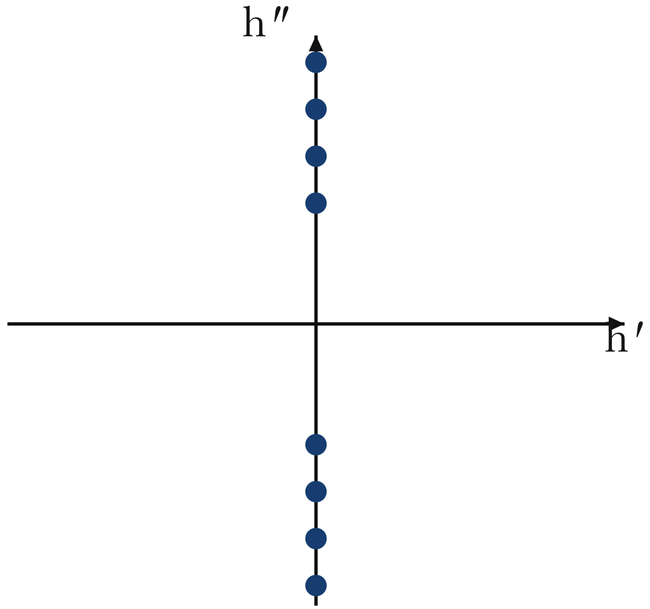
$Z = 0$

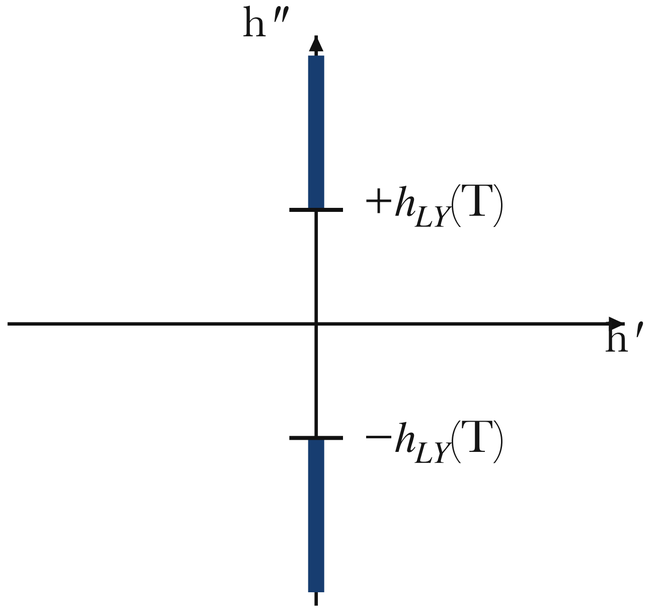
The sum returns to the origin

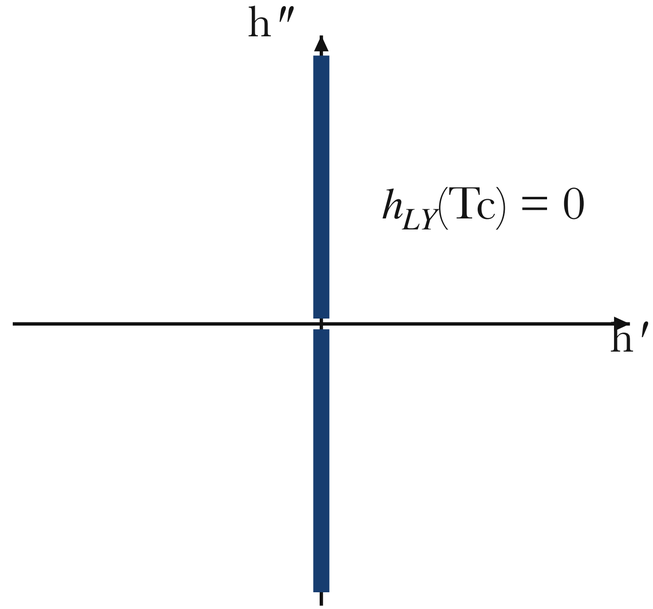
The complex roots of $Z(q)$ are the Lee–Yang zeros

Where the Lee–Yang edge comes from

Ferromagnetic Ising: zeros lie on $|q| = 1$, or imaginary h, with $q = \exp(-2h)$







Individual zeros

finite V, T > Tc

$f = -(T/V) \ln Z$

The edge

V → ∞, T > Tc

At the edge: a noninteger-power branch point

$$f_{\text{sing}} \sim (h - h_{\text{edge}})^{1+\sigma_{\text{LY}}}, \qquad M_{\text{sing}} \sim (h - h_{\text{edge}})^{\sigma_{\text{LY}}}$$

A real transition

V → ∞, T → Tc

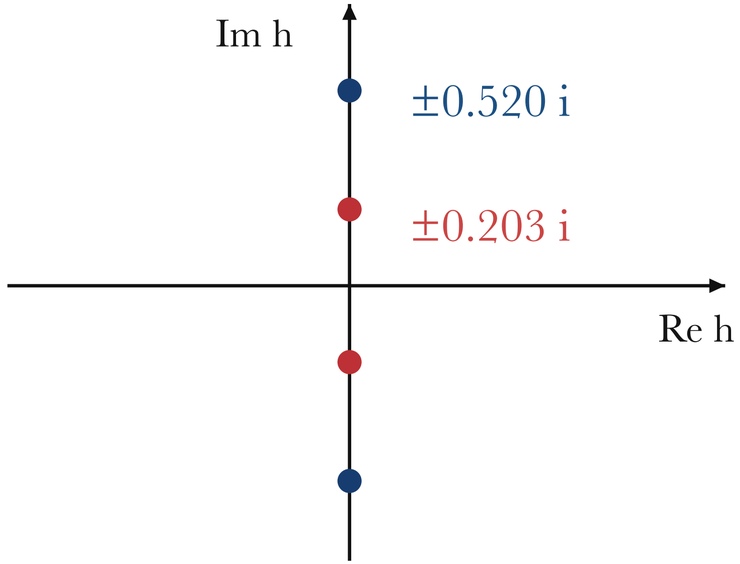
Lee & Yang (1952). C. Schmidt, PoS(EuroPLEx2023)037. Fisher, PRL 40 (1978) 1610.

An off-axis edge can sharpen a smooth crossover

$$m(h) = \frac{\sinh h}{\sqrt{\sinh^2 h + e^{-4K}}}$$

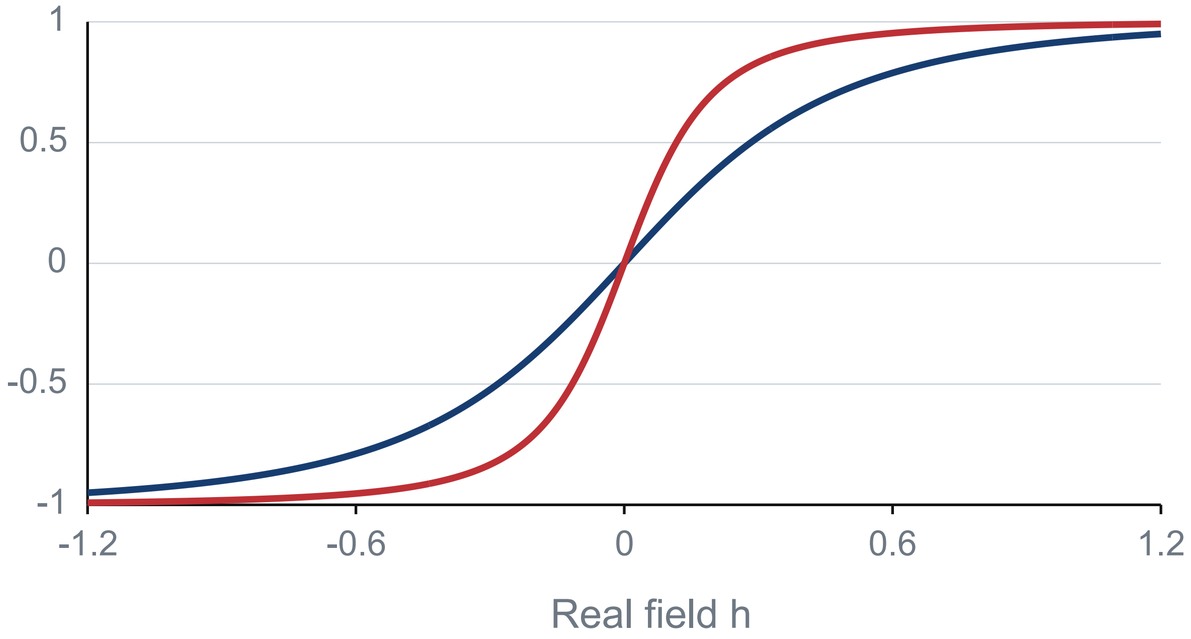
$$h_{\text{edge}} = \pm i \arcsin(e^{-2K})$$

Complex field



K = 0.35 K = 0.80

Magnetization at real field



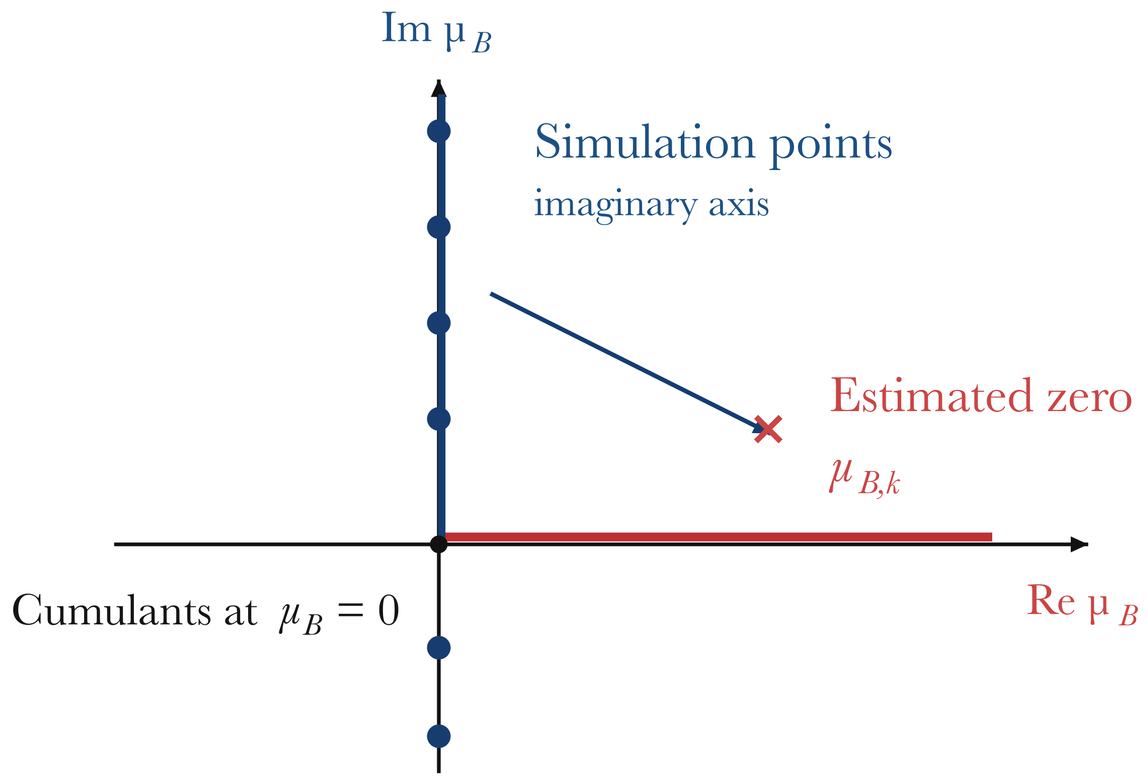
Slope at h = 0: 2.01 → 4.95

Closer complex edge → sharper crossover, with no real-axis singularity

Exact infinite 1D Ising chain: h = H/T, K = J/T. Deger, Brange & Flindt, PRB 102 (2020) 174418.

How can lattice data locate a Lee–Yang zero?

Where we simulate and what we infer



The estimated zero can have real and imaginary parts

Baryon-number fluctuations

$$\chi_n^B = \frac{1}{VT^3}\frac{\partial^n \ln Z}{\partial u^n}, \qquad u = \frac{\mu_B}{T}$$

Near a simple zero u_k

$$Z \sim (u - u_k) \quad \Longrightarrow \quad \frac{\partial \ln Z}{\partial u} \sim \frac{1}{u - u_k}$$

Rational reconstruction

Fit both lattice inputs to estimate
the leading zero in the complex plane

How the edge connects to the chiral transition

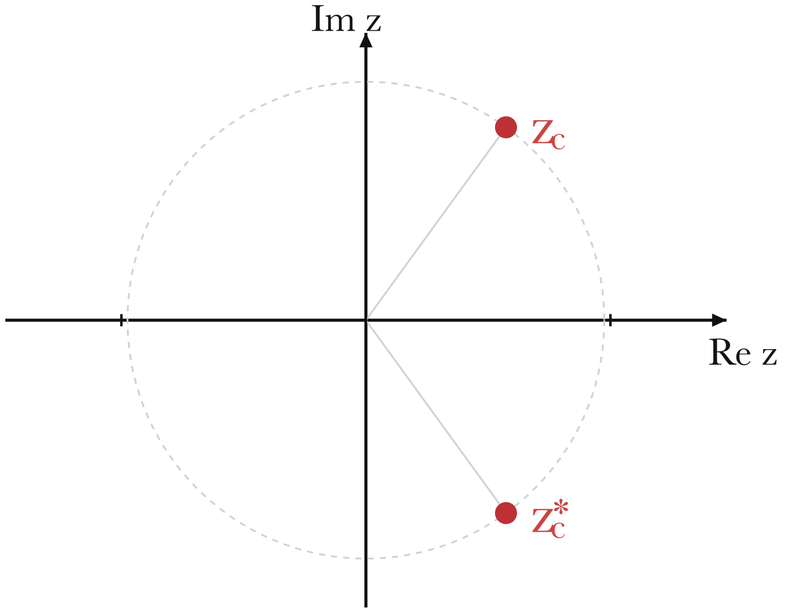
$$f_s \sim H^{1+1/\delta}\Phi(z), \qquad H = \frac{m_l}{m_s^{\mathrm{phys}}}$$ QCD variables → scaling variable z

- For real μ_B: $T_c(\mu_B)$ is the chiral-limit critical temperature, defined at H = 0.

$$z(T_i, \mu_B; H) = z_0 H^{-1/(\beta\delta)}\left[\frac{T_i}{T_c(\mu_B)} - 1\right]$$

The light-quark mass H breaks chiral symmetry, μ_B enters the temperature-like field

- In the complex plane of μ_B → complex plane of z



$$z_c = |z_c| e^{i\pi/(2\beta\delta)}$$ O(2): $|z_c|$ = 1.95(7), βδ = 1.6664(5)

$$z\left(T_i; \mu_{B,c}(T_i); H\right) \longrightarrow z_c$$

H → 0: edges reach $T_c(\mu_B)$. Physical H: complex edges, real crossover.

HTD, S. Mukherjee, P. Petreczky, Kai-Fan Ye, arXiv:2608.05752

From Chiral universality to the QCD crossover at finite density

Connection between LY edge and chiral universality

$$z_c = z_0 H^{-1/(\beta\delta)} \left[\frac{T}{T_c(\mu_B)} - 1 \right] \quad \longleftarrow \quad z = z_0 H^{-1/(\beta\delta)} \left[\frac{T}{T_c(\mu_B)} - 1 \right]$$

- QCD map function: $T_c(\mu_B) = T_c^0 g(x), \qquad x \equiv \frac{\mu_B}{T_c^0}$

- Chiral crossover transition: $T_{\rm pc}(\mu_B) = T_c(\mu_B)\left[1 + \frac{z_{\rm pc}}{z_0} H^{1/(\beta\delta)}\right] = T_c^0 \left[1 + \frac{z_{\rm pc}}{z_0} H^{1/(\beta\delta)}\right] g\left(\frac{\mu_B}{T_c^0}\right)$

$$= T_{\rm pc}(0)\, g\left(\frac{\mu_B}{T_c^0}\right)$$

- Fit g(x) to the input zeros, then evaluate it on the real axis

Parameterization of the map function (M1)

$$g(x) = e^{-(a^2 x^2 + b^2 x^4)}$$

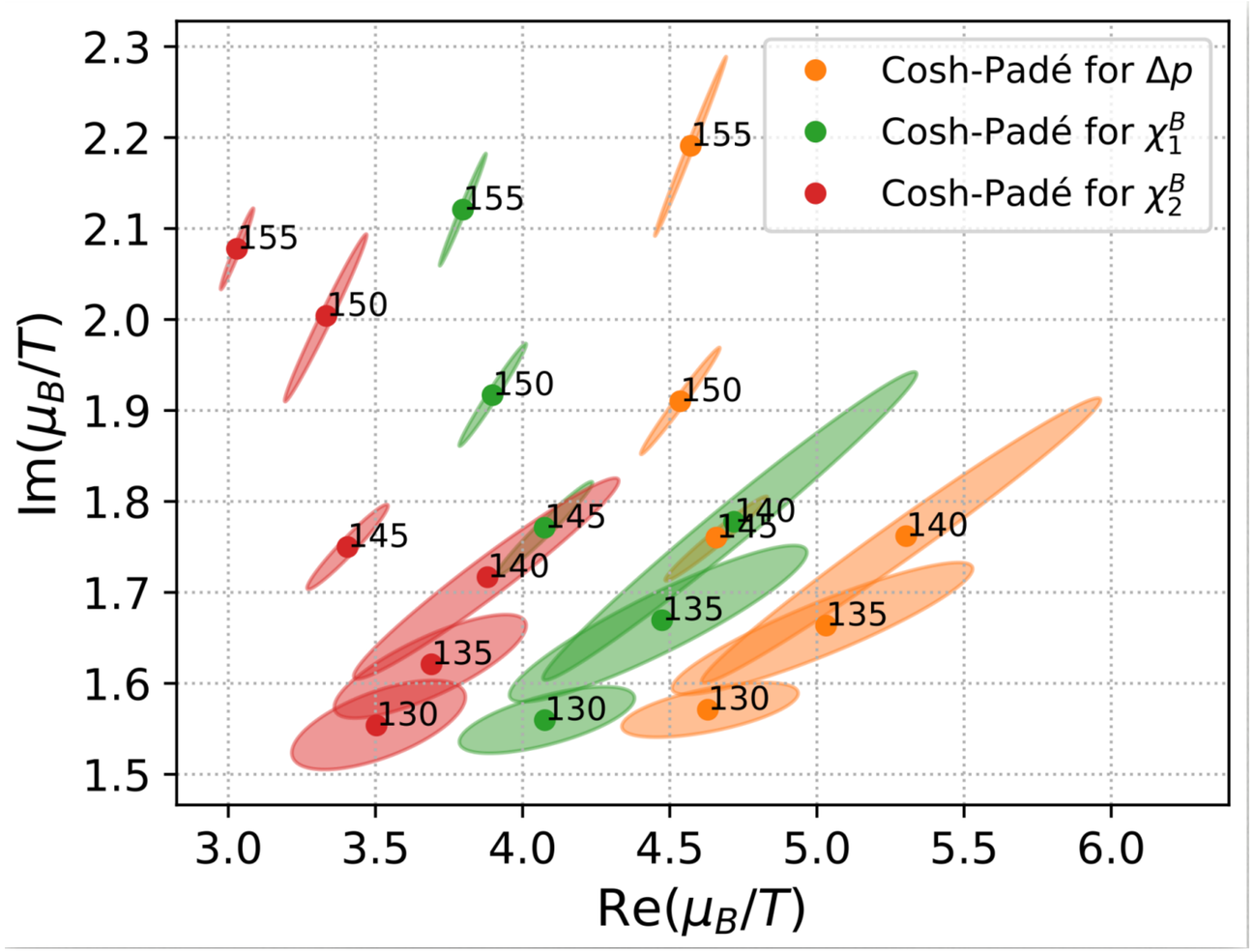
4 fit parameters

$$\{T_c^0,\ z_0,\ a,\ b\}$$

HTD, S. Mukherjee, P. Petreczky, Kai-Fan Ye, arXiv:2608.05752

WB provides the complex zeros for our reconstruction

Imaginary-μ_B data + high-order cumulants → rational reconstruction → leading zeros



Physical masses: H = 1/27

$16^3 \times 8$ lattice

ΔP: reference input

χ_1^B and χ_2^B: cross-checks

Finite-volume zeros
used as edge proxies

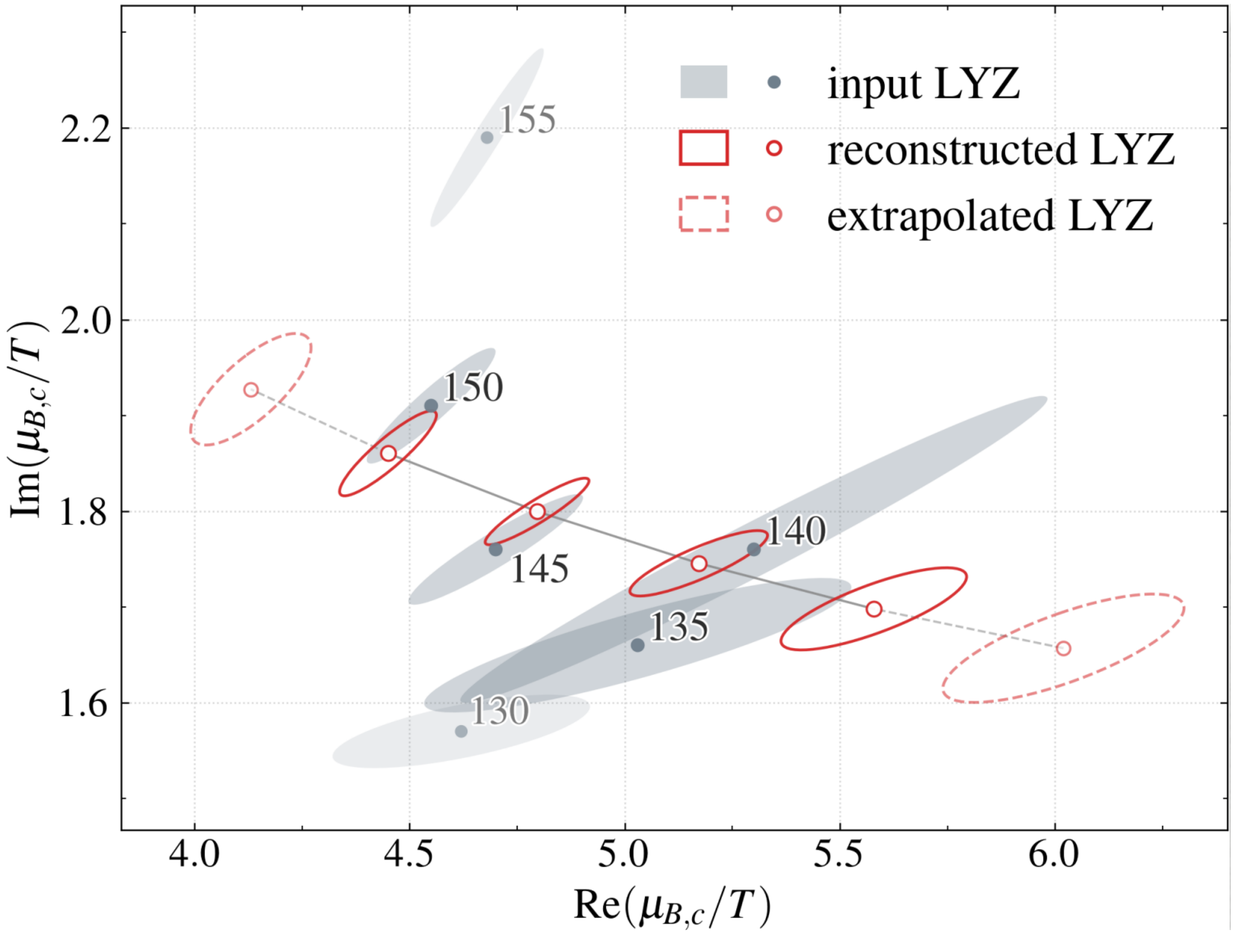
4 temperatures in the baseline fit

135, 140, 145, 150 MeV

Adam et al. [WB], PRD 113 (2026) 074525

Apply the common map to the WB zero locations

4 complex inputs → 8 real coordinates → 4 common fit parameters



Ellipses show complex-zero uncertainties

Baseline: ΔP + M1

$$g(x) = e^{-(a^2x^2+b^2x^4)}$$

Fit: 135, 140, 145, 150 MeV

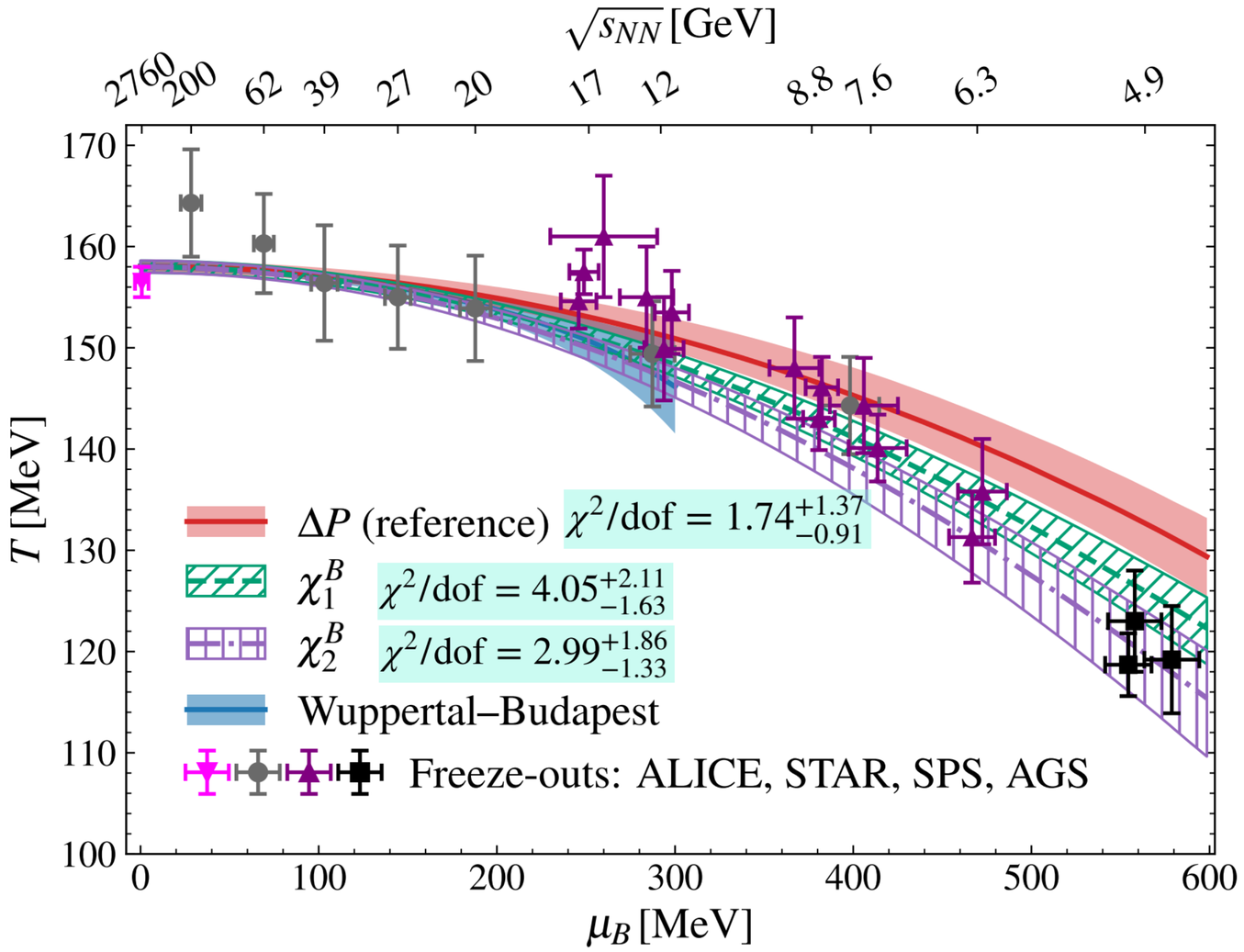
$$\chi^2/\mathrm{dof} = 1.74^{+1.37}_{-0.91}$$

130 and 155 MeV

Predictions outside the fit

Solid: fitted temperatures
Dashed: extrapolation tests

The reconstructed physical-mass crossover line



$$T_{\mathrm{pc}}(\mu_B) = T_{\mathrm{pc}}(0)\, g(x)$$

$$g(x) = e^{-(a^2x^2+b^2x^4)}$$

ΔP: reference reconstruction

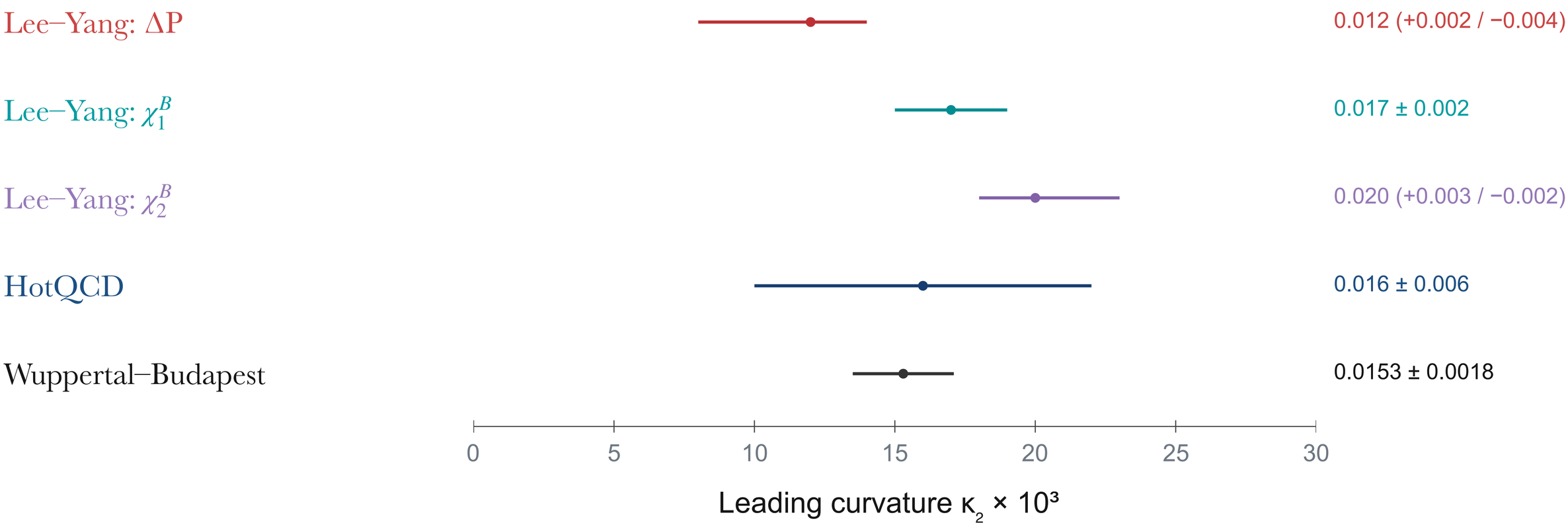
Agreement with lattice at small μB

Observable dependence grows at larger μ_B

HTD, S. Mukherjee, P. Petreczky, Kai-Fan Ye, arXiv:2608.05752

The leading curvature provides an independent test

$$\frac{T_{\rm pc}(\mu_B)}{T_{\rm pc}(0)} = 1 - \kappa_2 \left(\frac{\mu_B}{T_{\rm pc}(0)} \right)^2 + \cdots$$



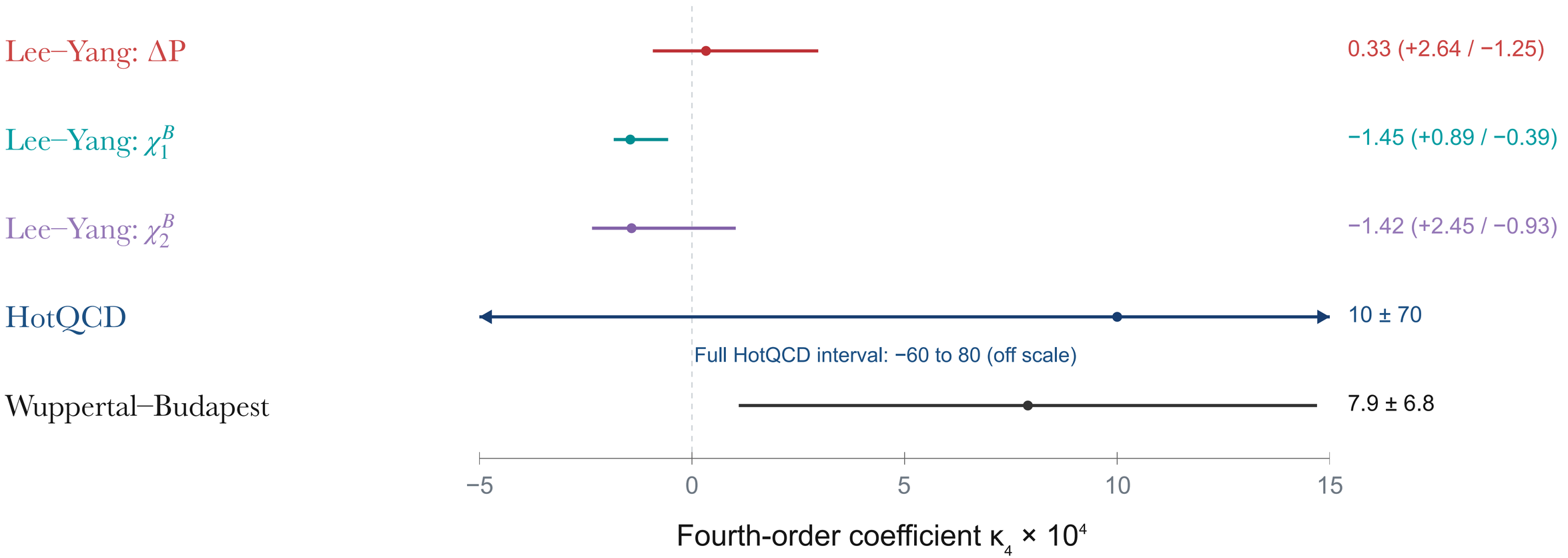
LY + HotQCD: μQ = μS = 0. WB: nS = 0, μQ = 0.

HotQCD, PLB 795 (2019) 15. WB, PRL 125 (2020) 052001

Fourth-order curvature is less precisely constrained

$$\frac{T_{\rm pc}(\mu_B)}{T_{\rm pc}(0)} = 1 - \kappa_2 \left(\frac{\mu_B}{T_{\rm pc}(0)}\right)^2 - \kappa_4 \left(\frac{\mu_B}{T_{\rm pc}(0)}\right)^4 + \cdots$$

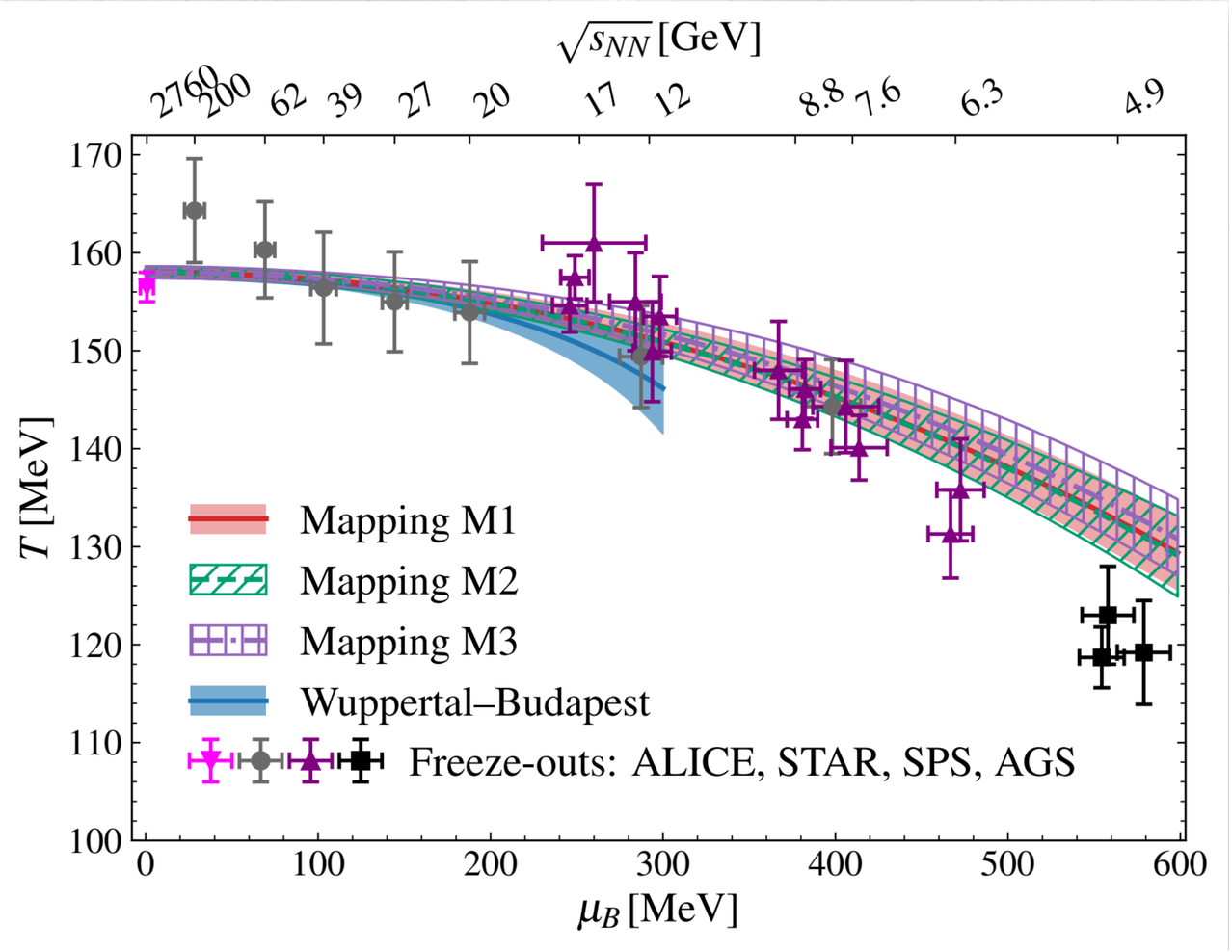
All values × 10^{-4}; WB converted to the convention above



LY + HotQCD: μQ = μS = 0. WB: nS = 0, μQ = 0.

Ding et al., arXiv:2608.05752. HotQCD, PLB 795 (2019) 15. WB, PRL 125 (2020) 052001

The result is stable across three mapping choices



$$g(x) = \exp[-F(x)], \qquad x = \mu_B/T_c^0$$

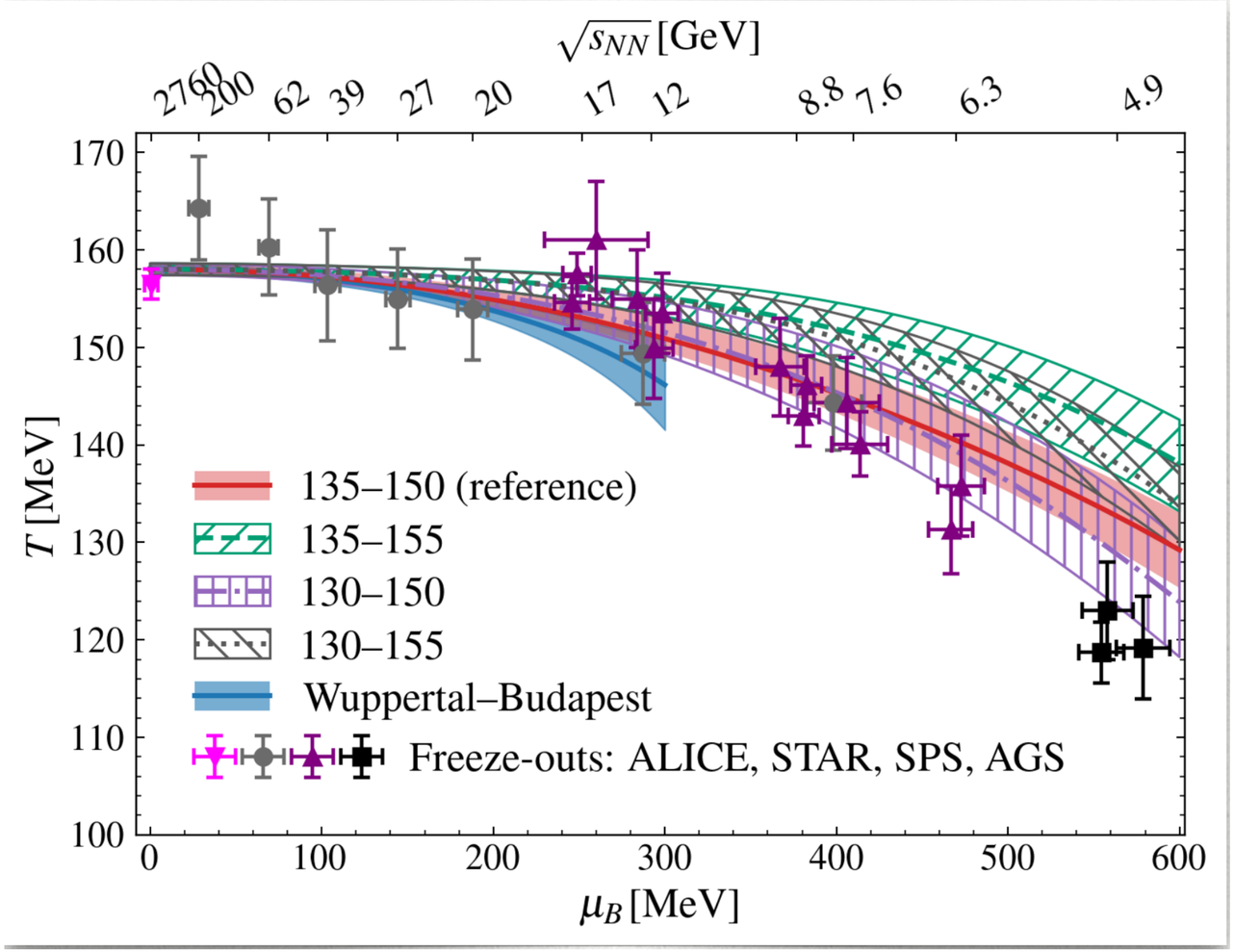
$$\text{M1}: \quad F(x) = a^2x^2 + b^2x^4$$

$$\text{M2}: \quad F(x) = a^2x^2 - abx^4 + \frac{b^2}{3}x^6$$

$$\text{M3}: \quad F(x) = \frac{a^2x^2 + b^2x^4}{1 + c^2x^2}$$

Even in μ_B, g(0) = 1; positive and decreasing on the real axis

The temperature window tests the scaling description



Median fit quality

T window [MeV]	χ^2 / dof
135–150	1.74
130–155	4.42
130–150	3.79
135–155	2.68

Broader windows lower T_c^0 to about 110 MeV and increase χ^2/dof

Recent theoretical predictions/estimates of CEP

- $T^{\mathrm{CEP}} = 114.3 \pm 6.9$ MeV
- $T^{\mathrm{CEP}} = 105^{+8}_{-18}$ MeV
- $T^{\mathrm{CEP}} < 103$ MeV w. 84% prob. or No CEP

Current LQCD simulations at $T \geq 120$ MeV

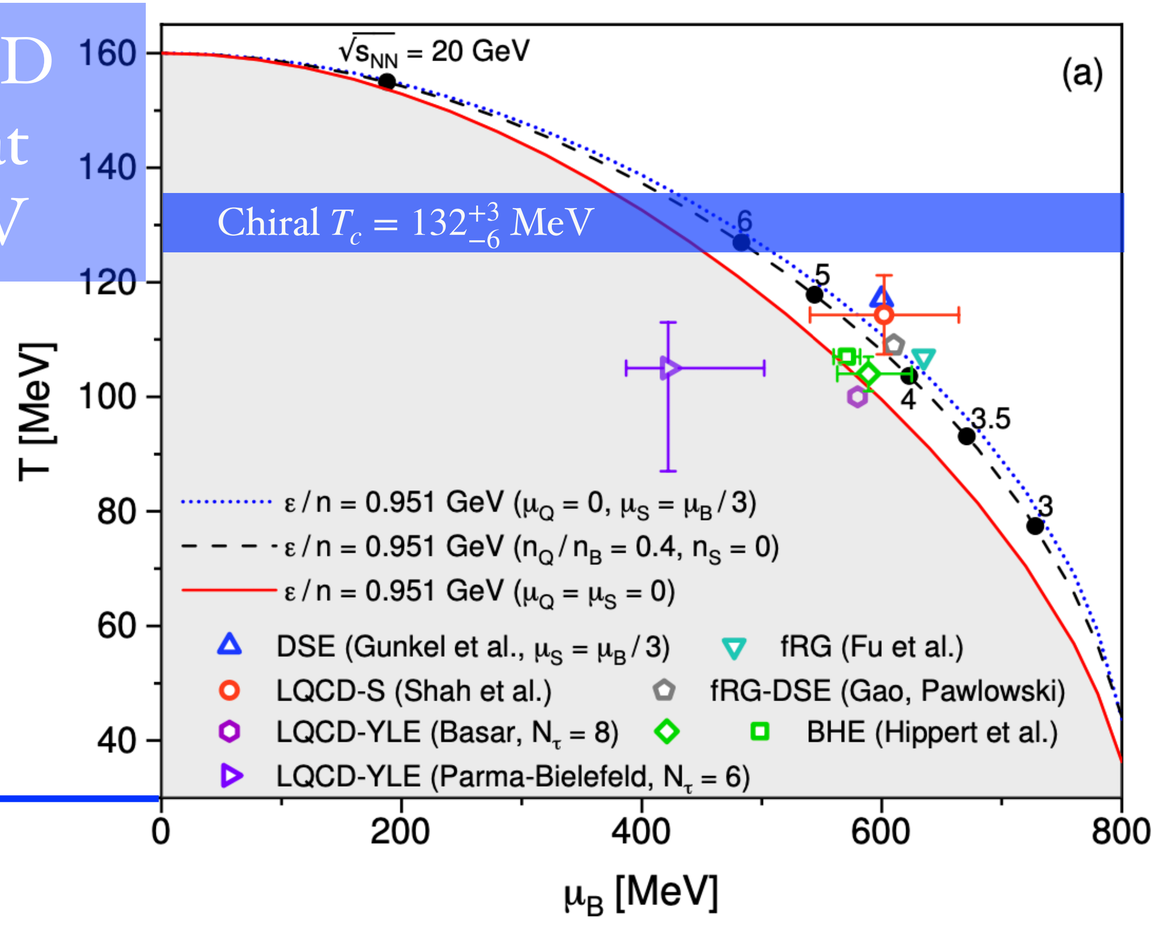
- Recall recent estimates/predictions:

$$T_c^{\mathrm{CEP}} \approx 83 - 120 \text{ MeV}$$
$$\mu_{B,c}^{\mathrm{CEP}} \approx 387 - 664 \text{ MeV}$$

See more about FRG/DSE from Jan & Christian today

- How about perform a direct LQCD simulations in the currently predicted T_c^{CEP} region? E.g. 108 MeV

$Im(\mu_B)$



Lysenko et al., arXiv:2408.06473, *Phys.Rev.C* 111 (2025) 5, 054903

Lattice setup at T≈108 MeV

- N_f=2+1 QCD on 20^3x10 lattices with at T=107.7 MeV using HISQ fermions at the physical point with $\mu_u = \mu_d = \mu_s = \mu_B/3$
- 24 values of $i\mu_B \in [0, i\pi]$ each for χ^B_{1-4}
- 400k configurations for zero chemical potential, 200k for others
- Additional 32^3x10 lattices generated to check the volume dependence

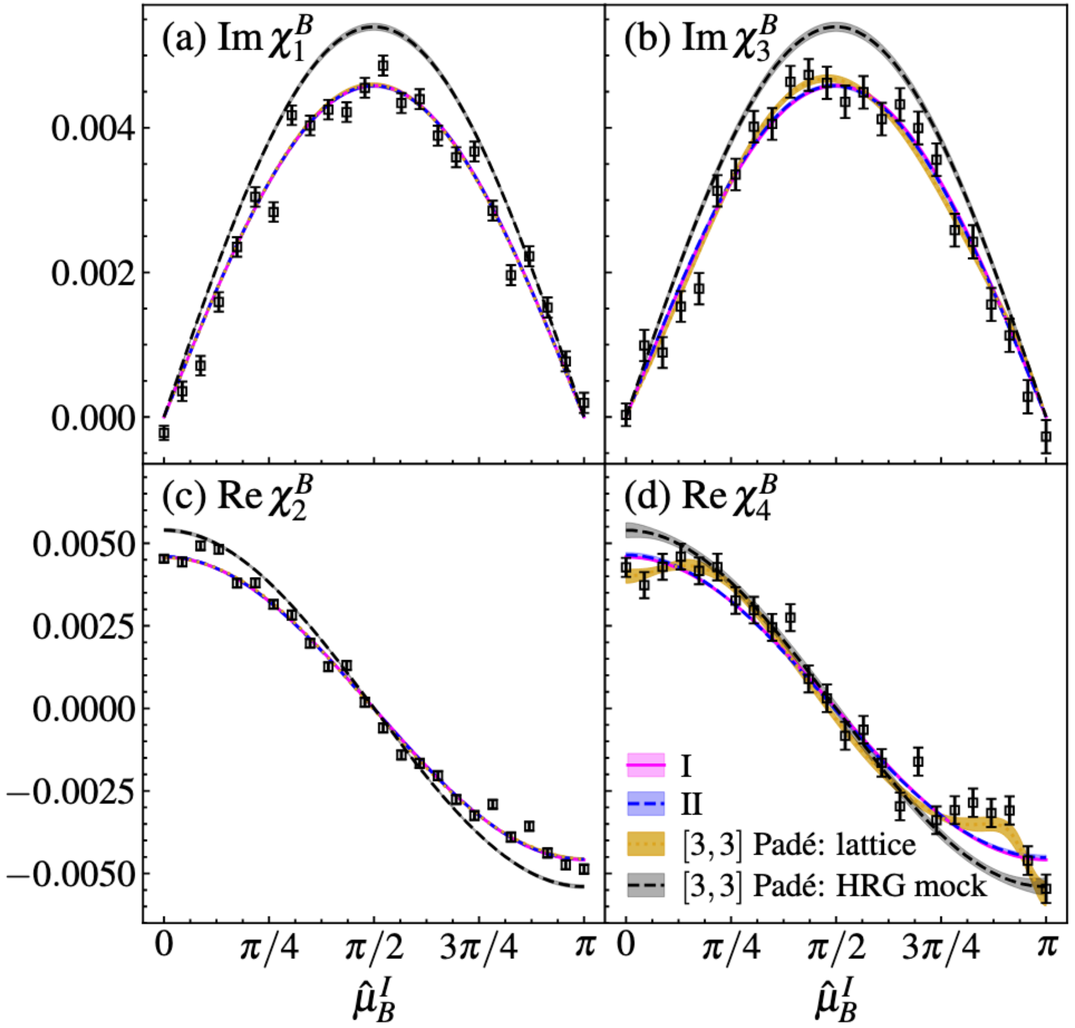
NSCC Nuclear Science Computing Center at CCNU + SUMMIT

Multi-point Padé fits

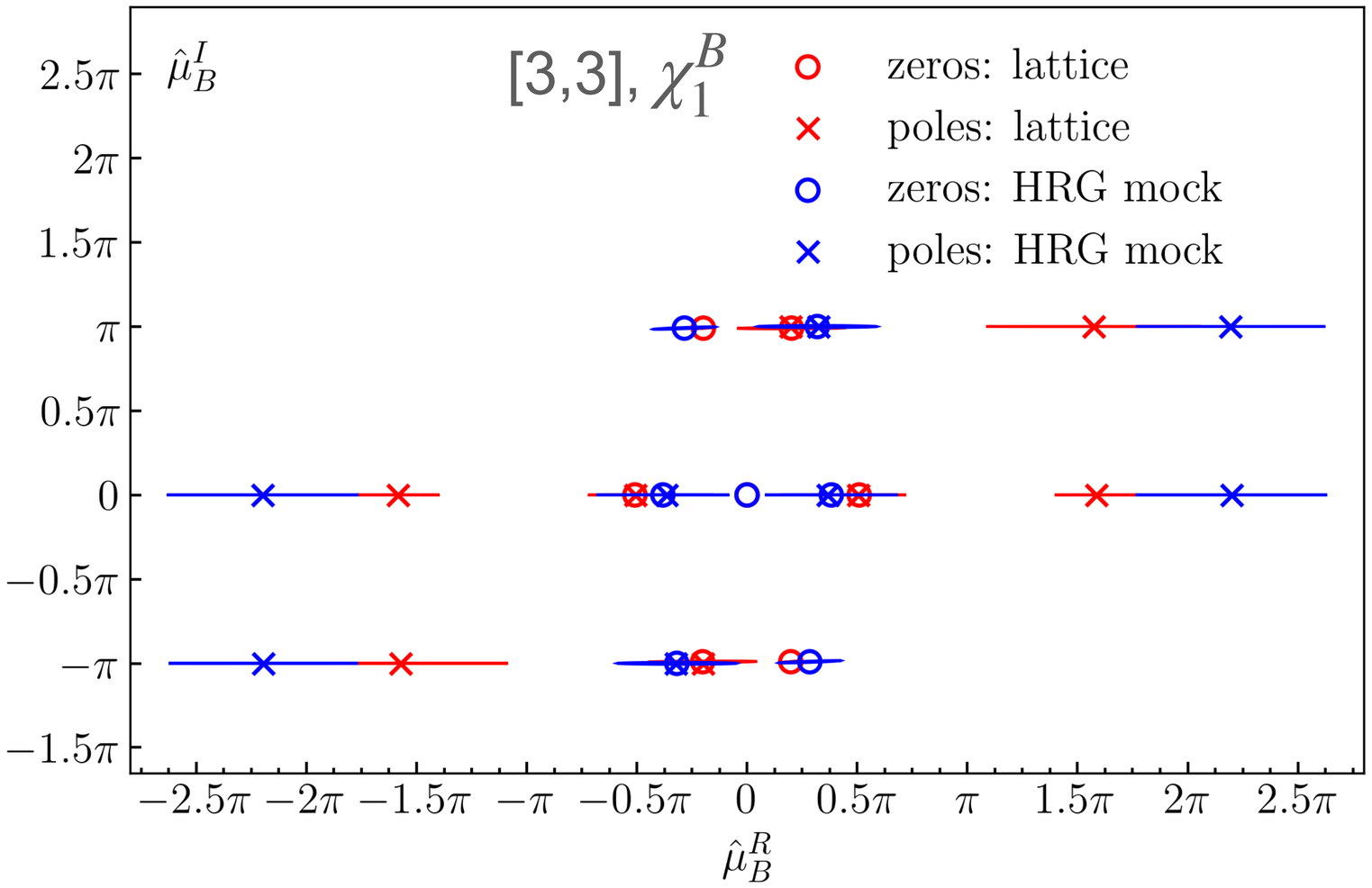
$$P(x) \equiv R_k^m(x) = \frac{\sum_{i=0}^{m} a_i x^i}{1 + \sum_{j=1}^{k} b_j x^j}, x = \cosh(\mu_B) - 1$$

- Generate N_{boot} bootstrap samples by resampling $N_{conf,i}$ configurations allowing replacement for each one of 24 discrete values of $\mu_{B,i}$, and compute mean value of χ^B_{1-4} at $\mu_{B,i}$ within each bootstrap sample
- Joint fit to χ^B_n *with* $\partial^n P(x)/\partial\mu_B^n$ *with n=1-4 in each bootstrap sample with covariance matrix obtained from the original data sets*
- Final uncertainties from 68% confidence interval over bootstrap fits

[3,3]



Zero/poles extracted from Padé [3,3] analyses



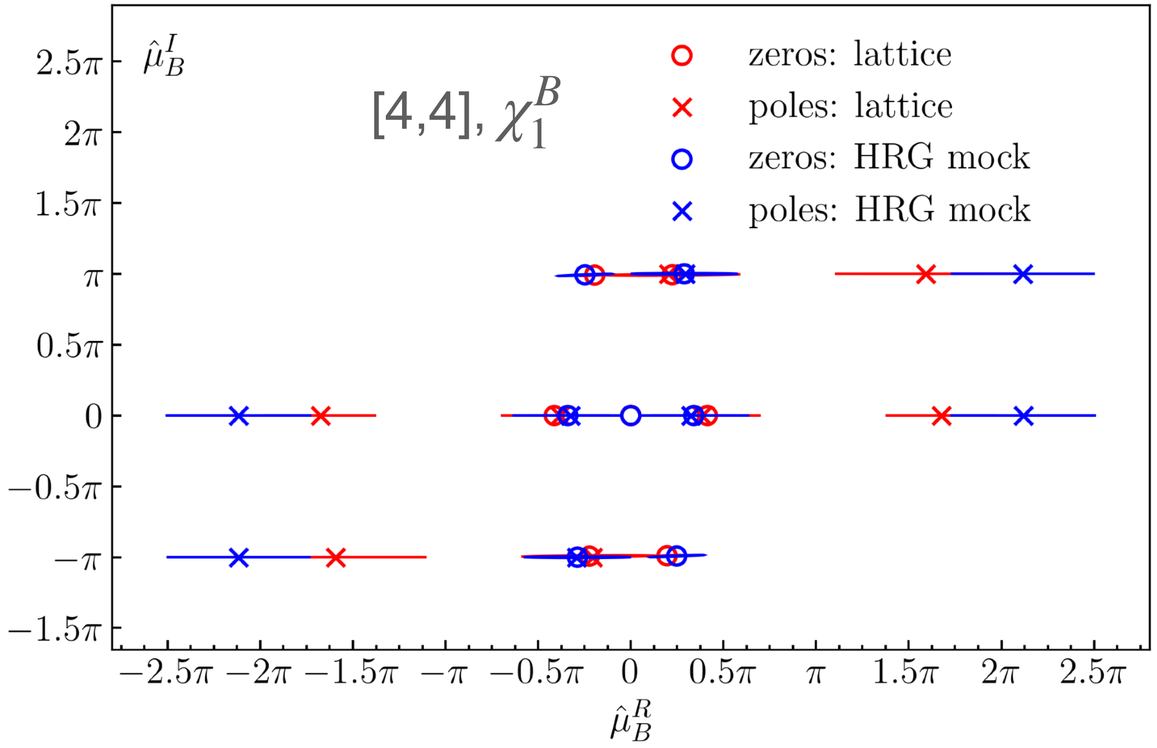
$$P(x) = \frac{\sum_{i=0}^{m} a_i x^i}{1 + \sum_{j=1}^{n} b_j x^j}$$

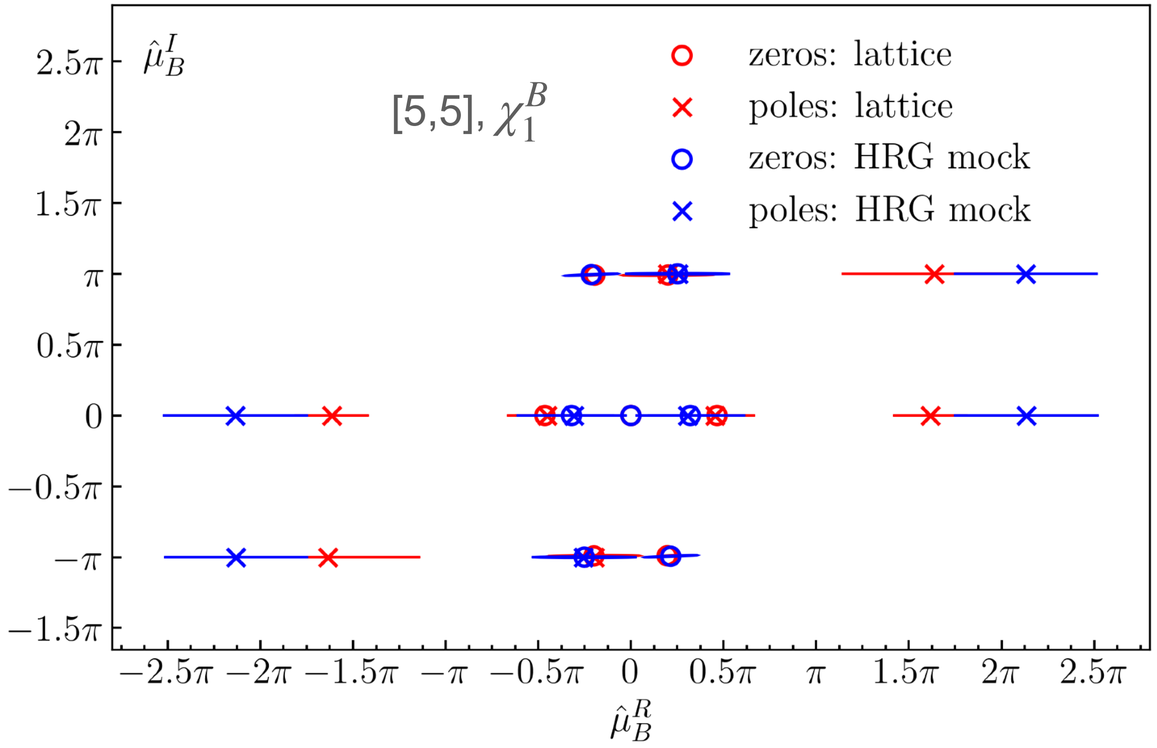
$$\chi_1^B = \partial P(x)/\partial \mu_B$$

Zeros: roots of numerator
Poles: roots of denominator

- No uncanceled poles
- Similar pattern between Lattice and HRG mock

Zero/poles extracted from higher order Padé analyses

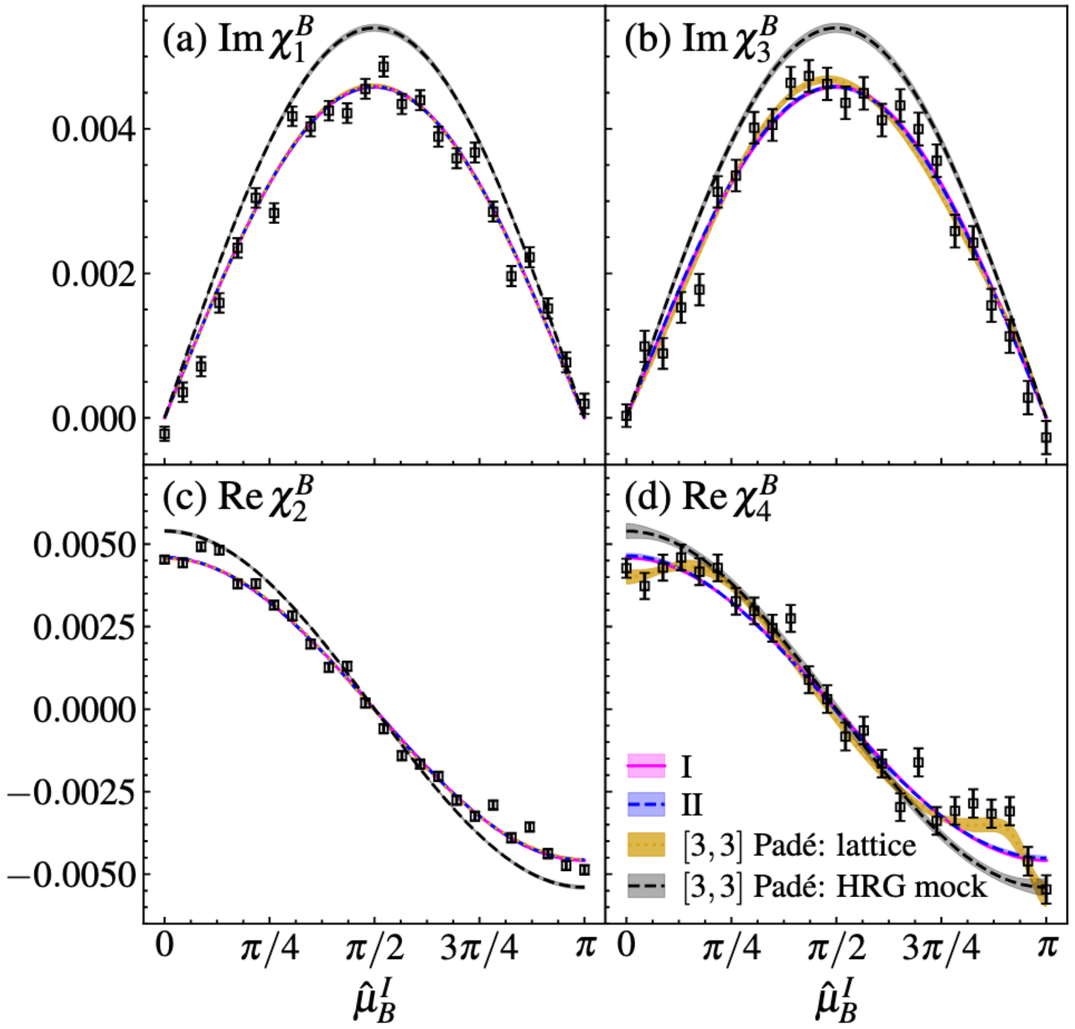




Similar observation as in the case of Padé [3,3]

Kai-Fan Ye et al., [Bielefeld-BNL-CCNU], in preparation

Fits with physical-motivated non-critical ansatz



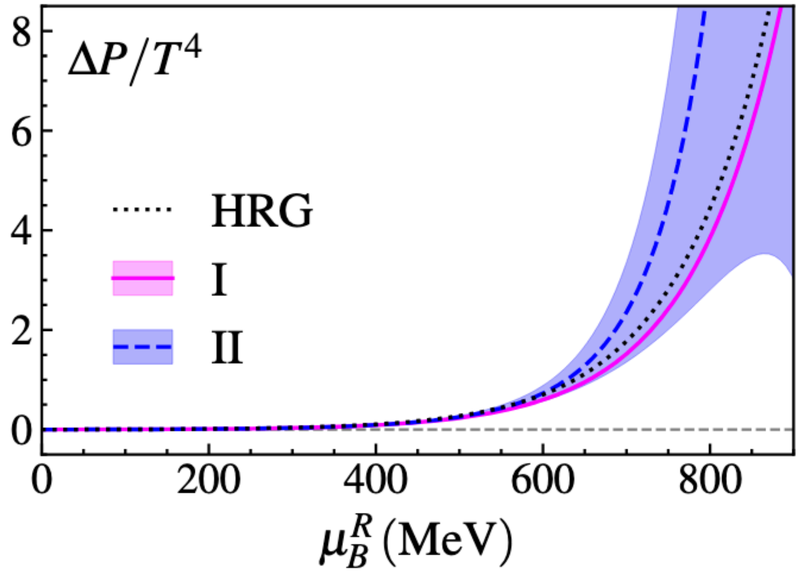
Non-critical ansatz for pressure:

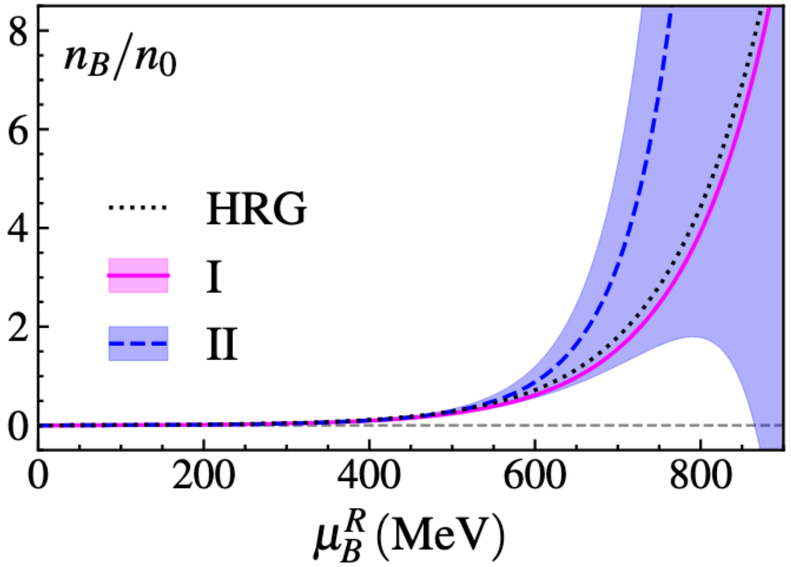
Ansatz I: $f(\mu_B) = A\cosh(\mu_B)$

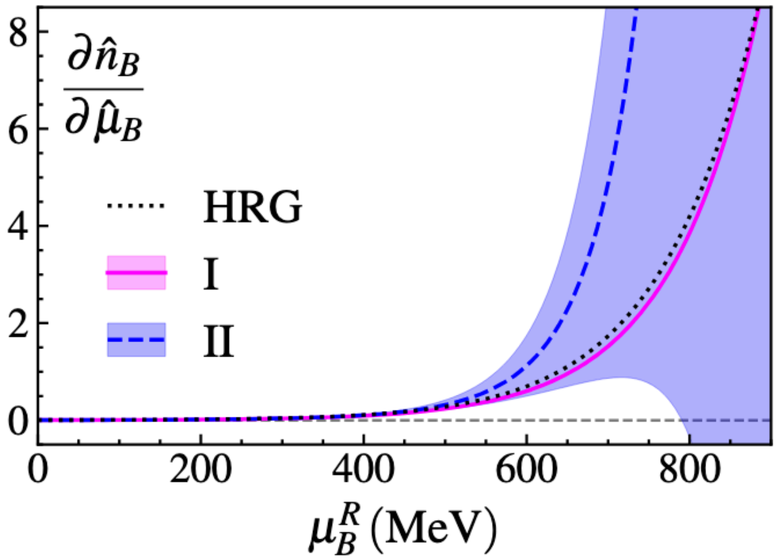
Ansatz II: $f(\mu_B) = A\cosh(\mu_B) + B\cosh(2\mu_B)$

	Lattice QCD Data			
	All 24 points		Random 12 points	
	Ansatz I	Ansatz II	Ansatz I	Ansatz II
Parameters				
A $(\times 10^{-3})$	4.584(25)	4.582(25)	4.584(62)	4.584(63)
B $(\times 10^{-5})$	–	0.38(45)	–	0.4(10)
Statistics				
χ^2/d.o.f.	$4.20^{+0.40}_{-0.38}$	$4.22^{+0.40}_{-0.38}$	$4.17^{+0.75}_{-0.69}$	$4.20^{+0.75}_{-0.70}$
AICc	401^{+38}_{-36}	401^{+38}_{-36}	198^{+35}_{-32}	198^{+35}_{-32}

Analytic continuation to real μ_B at T=108 MeV



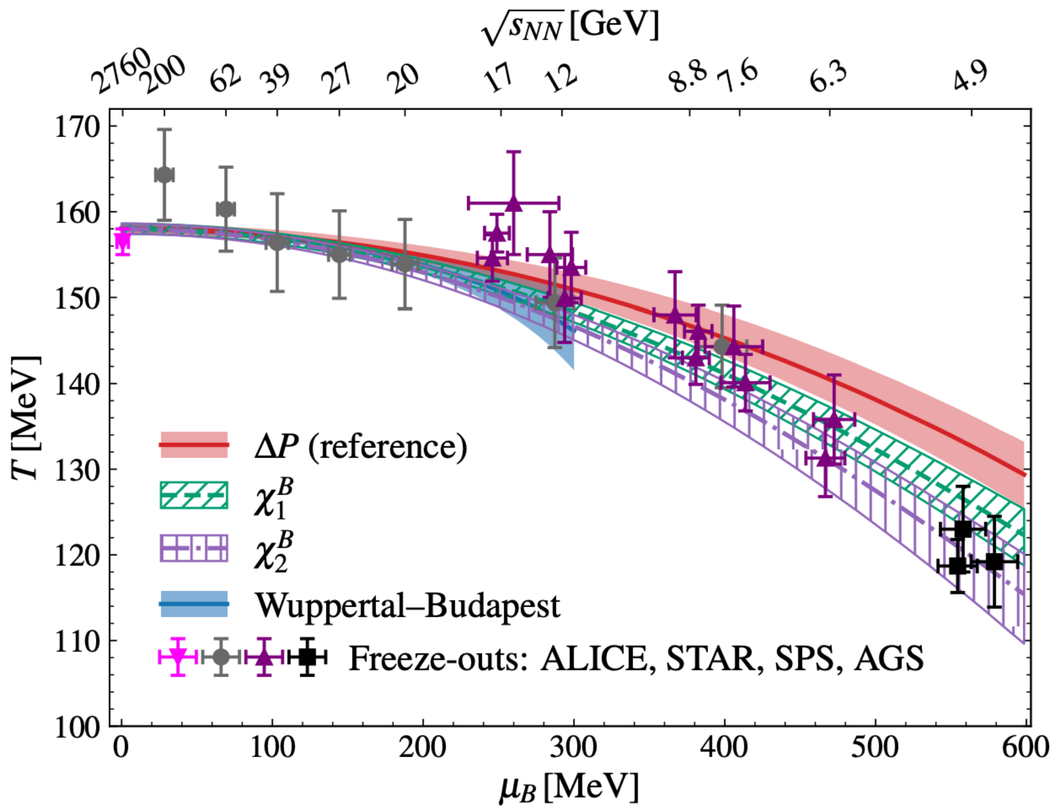




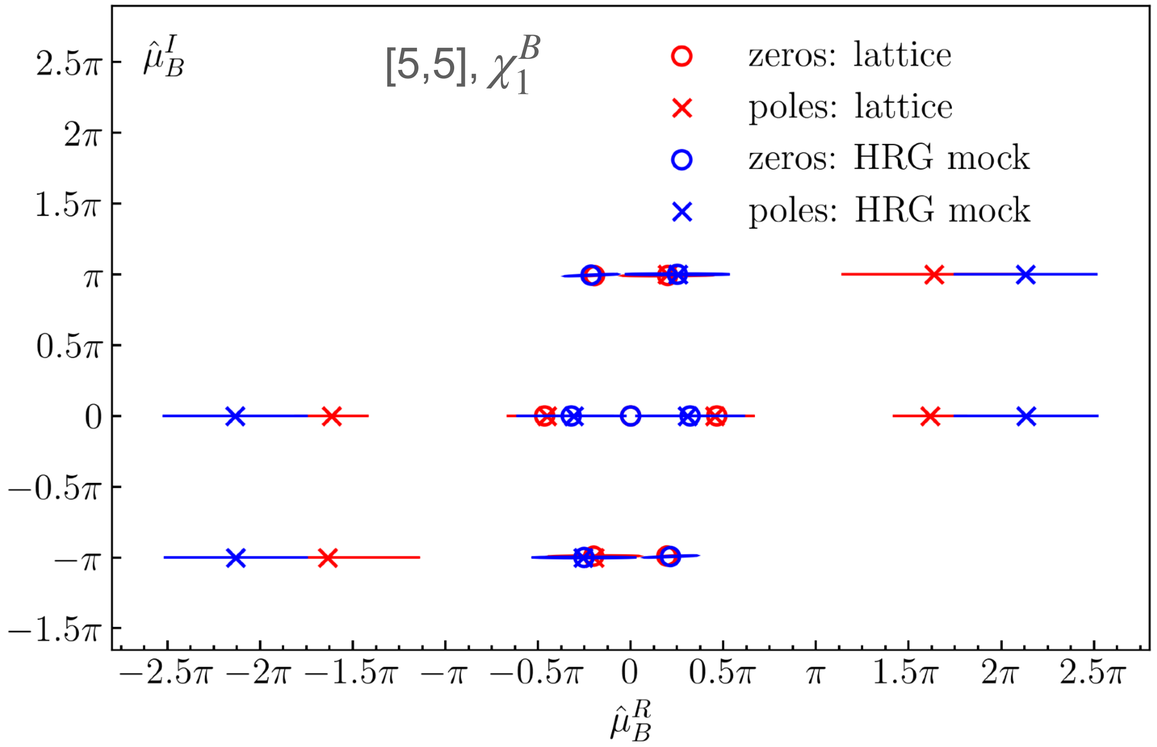
- Baryon number density $\hat{n}_B$ and $\partial \hat{n}_B / \partial \hat{\mu}_B$ shall be positive, which restricts $\mu_B^R \lesssim 800$MeV
- Results from ansatz I (non-interacting) and HRG are very much similar
- Results from ansatz II (interacting) differ from others at $\mu_B^R \gtrsim 500$MeV

Summary

Complex zeros constrain the real QCD crossover

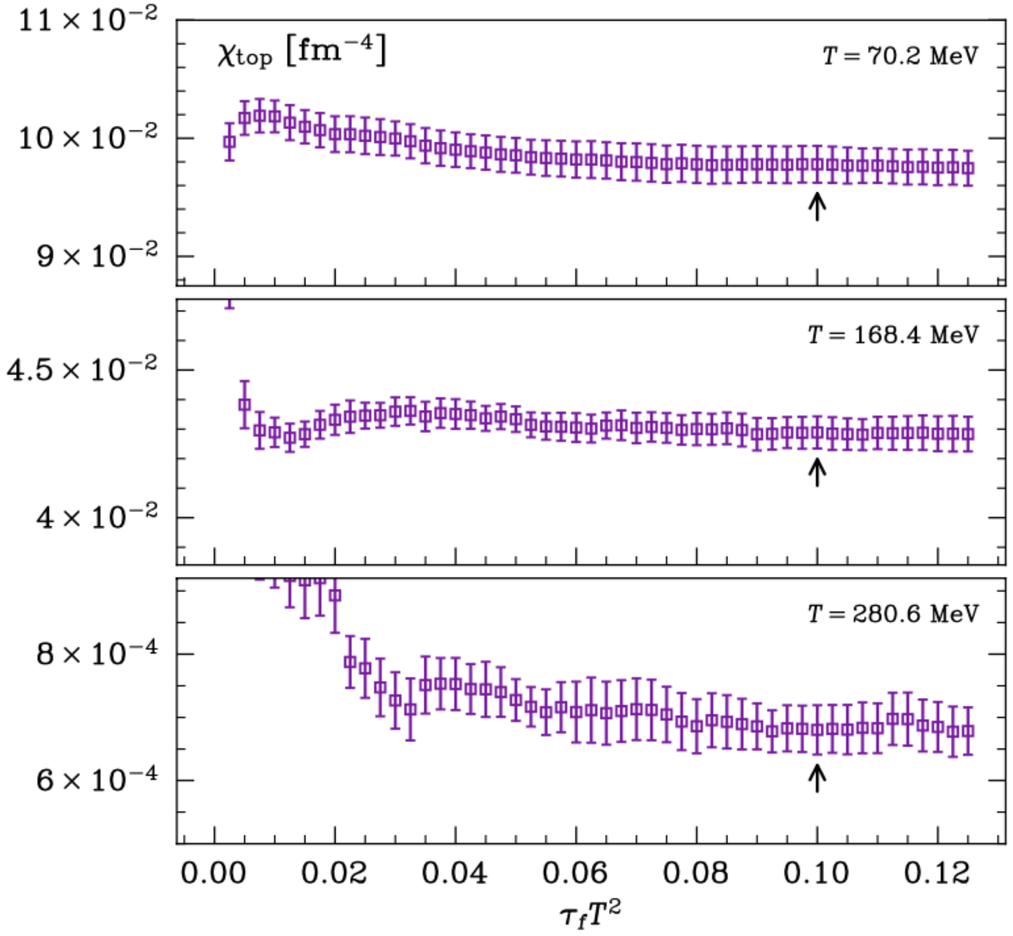


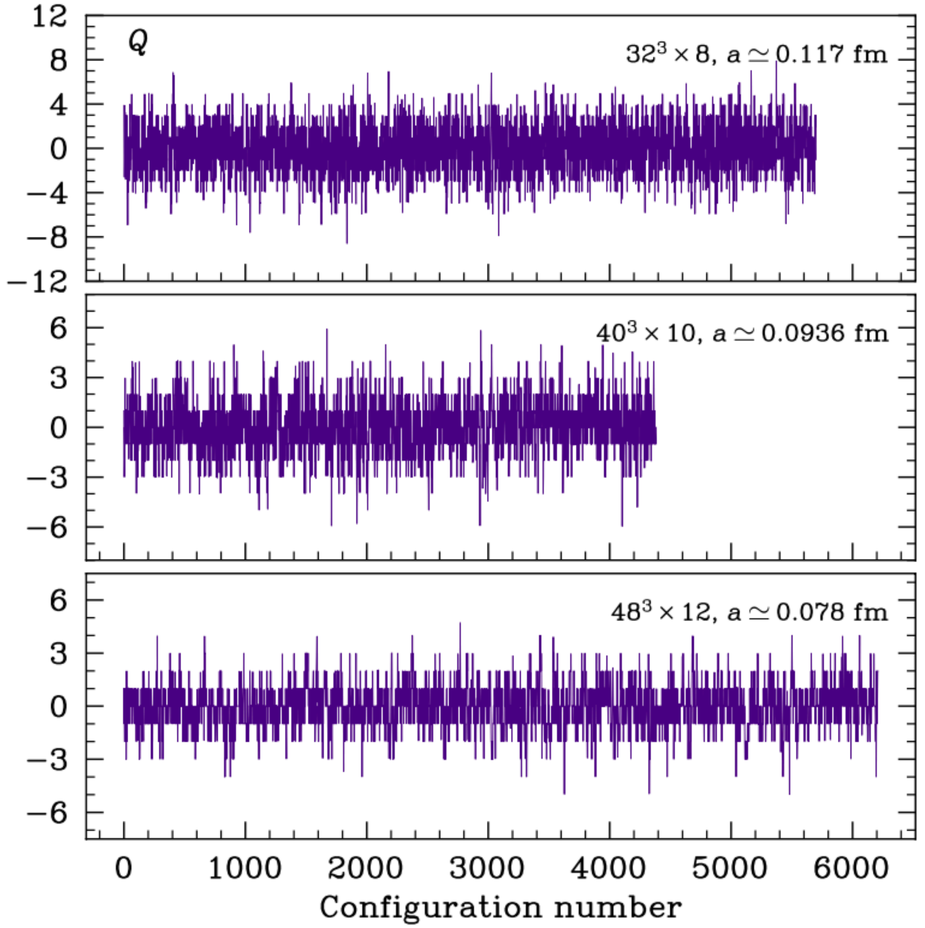
Lattice QCD data: comparable with HRG at T=108 MeV



Backup

Flow time dependence and time history of Q





Thermal scan and a continuum check

2+1-flavor HISQ, $m_\pi \approx 220$ MeV

$m_\ell = m_s/10$, physical m_s

$a \approx 0.117$ fm, spatial volume 32^3

N_τ	T [MeV]
24, 18, 16, 14	70.2, 93.6, 105.3, 120.4
12, 10, 8, 6	140.4, 168.5, 210.8, 280.9

Continuum check at T ≈ 211 MeV

$32^3 \times 8$ $40^3 \times 10$ $48^3 \times 12$

Matched masses and physical volume

Pseudocritical region: $T_{pc} \approx 170$ MeV

NSCC Nuclear Science Computing Center at CCNU

The chiral response measures a local mass slope

- Low temperature:
  chiral perturbation theory

$$\chi_{\text{top}}^{\text{LO}} = \frac{\Sigma}{2/m_\ell + 1/m_s}, \qquad C_{\text{top}}^{\text{LO}} = \frac{2m_s}{2m_s + m_\ell}$$

Grilli di Cortona et al., JHEP 01(2016) 034 ,Leutwyler & Smilga,, PRD46 (1992) 5607.

- High temperature:
  leading quadratic dependence

$$\chi_{\text{top}}(T) \propto m_\ell^2 \quad (m_s \text{ fixed}), \qquad C_{\text{top}} \simeq 2$$

Gross, Pisarski & Yaffe 1981, Schaffer & Shuryak 1998, Kanazawa & Yamamoto 2015



Chiral response
of QCD topology

$$C_{\text{top}}(T) = \left.\frac{\partial \ln \chi_{\text{top}}}{\partial \ln m_\ell}\right|_{T,V_4,m_s} \qquad \chi_{\text{top}} \propto m_\ell^p \quad \Longrightarrow \quad C_{\text{top}} = p$$



Mass derivative of O: $\dfrac{\partial O}{\partial x} = \lim_{\epsilon \to 0} \dfrac{O(x+\epsilon) - O(x)}{\epsilon}$

HTD, 顾锦彪, Hernández Hernández, 李胜泰 & 倪佳, arXiv:2611.xxxx

A single-ensemble estimator for the mass derivative

- QCD partition function: $Z = \int \mathcal{D}U\, e^{-S_g} \det(D + m_\ell)^2 \det(D + m_s)$

- Derivative of χ_{top} without additional situations on shifted quark masses

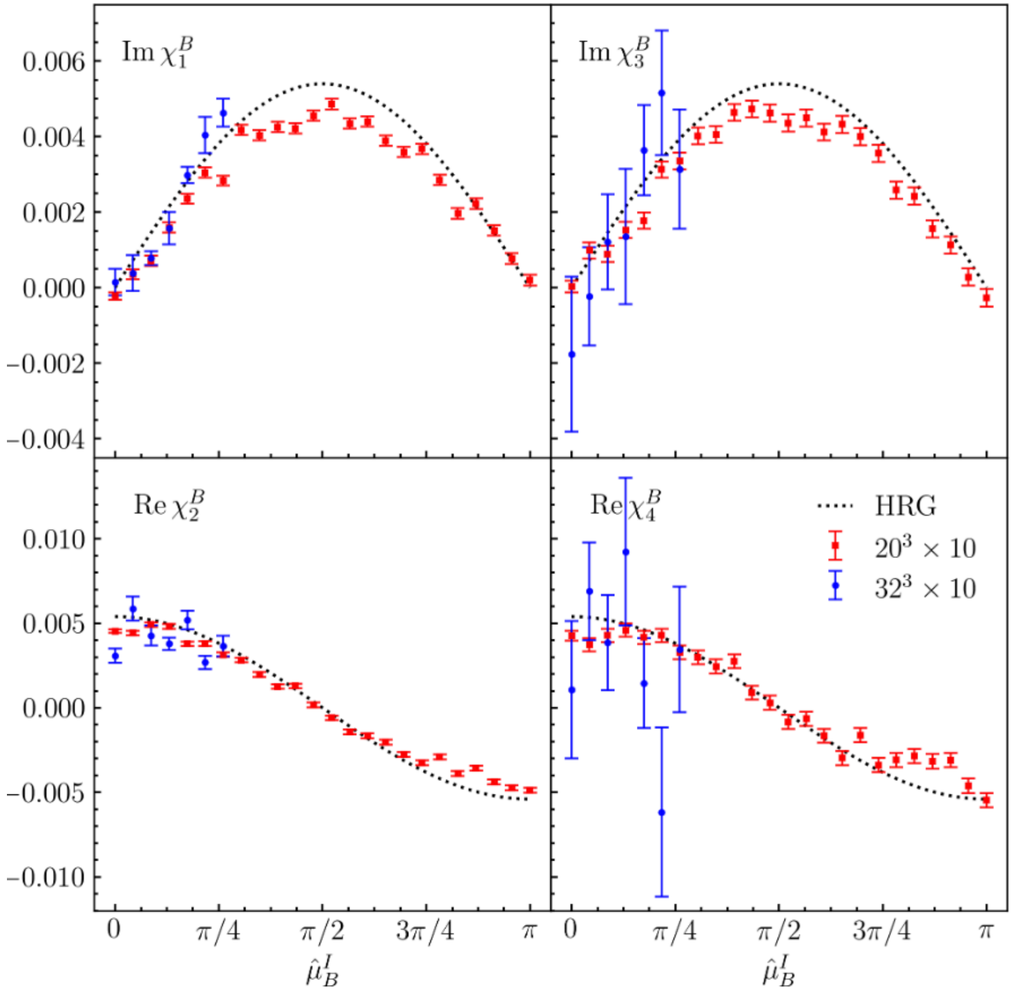
$$\frac{\partial \chi_{\text{top}}}{\partial m_\ell} = \frac{\langle Q^2 X_1 \rangle - \langle Q^2 \rangle \langle X_1 \rangle}{V_4} \qquad X_1 \equiv \partial_{m_\ell} \ln \det(D + m_\ell)^2 = 2\,\text{Tr}(D + m_\ell)^{-1}$$

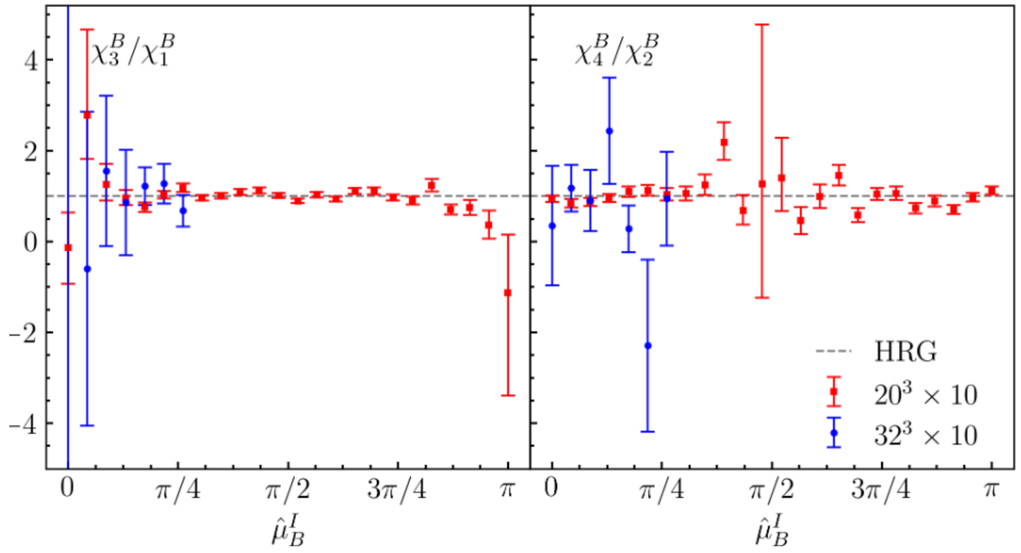
- The covariance supplies the response directly

$$C_{\text{top}} = m_\ell \frac{\langle Q^2 X_1 \rangle_c}{\langle Q^2 \rangle}$$

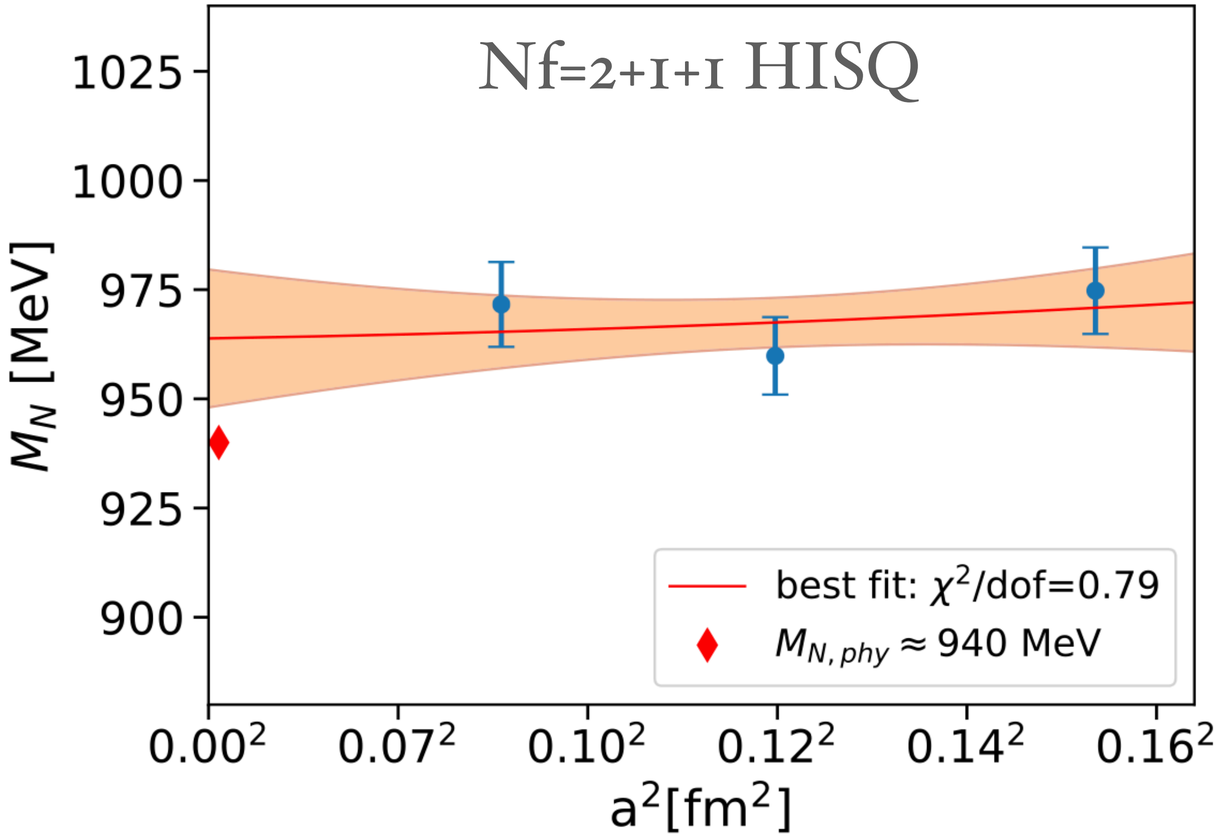
HTD, 顾锦彪, Hernández Hernández, 李胜泰 & 倪佳, arXiv:2611.xxxx

Volume dependences





Lattice cutoff effects



- Nt=10 at T=108 MeV⇒$a \approx 0.18$ *fm*
- proton mass is inflated by about 4-5%, ~980MeV at $a \approx 0.18$ *fm*, as estimated the from the difference in A fit parameter

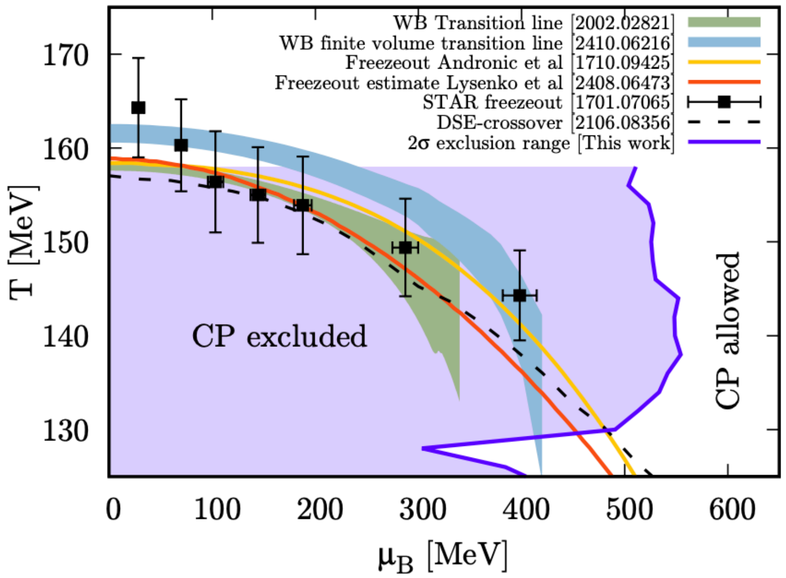
$$A_{LAT}=4.584(25)$$
$$A_{HRG}=5.397(30)$$

- Consistent with direct computation in Nf=2+1+1 QCD

Yin Lin et al., *Phys.Rev.D* 103 (2021) 3, 034501

Recent results on the CEP search in Lattice QCD

Contour of constant entropy



No CEP at $\mu_B < 450$ MeV at the 2σ level

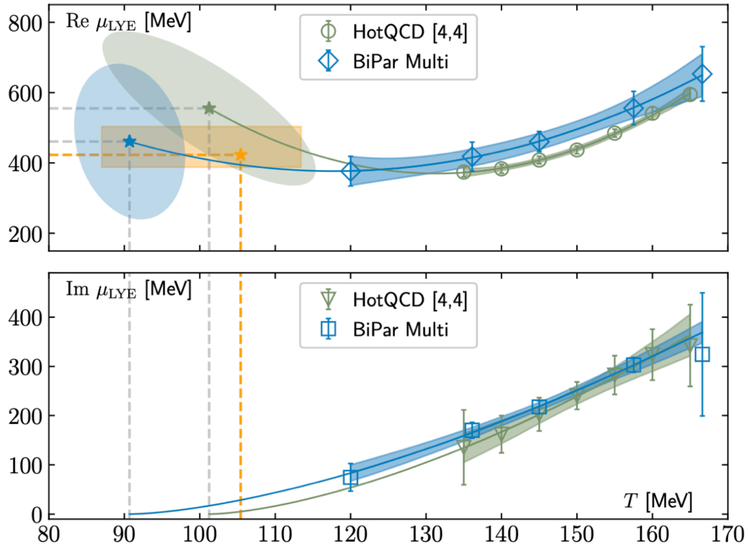
Borsányi et al., arXiv:2502.10267

$T^{\mathrm{CEP}} = 114.3 \pm 6.9$ MeV

$\mu_B^{\mathrm{CEP}} = 602.1 \pm 62.1$ MeV

Shah et al., arXiv:2410.16206

Lee-Yang edge singularity

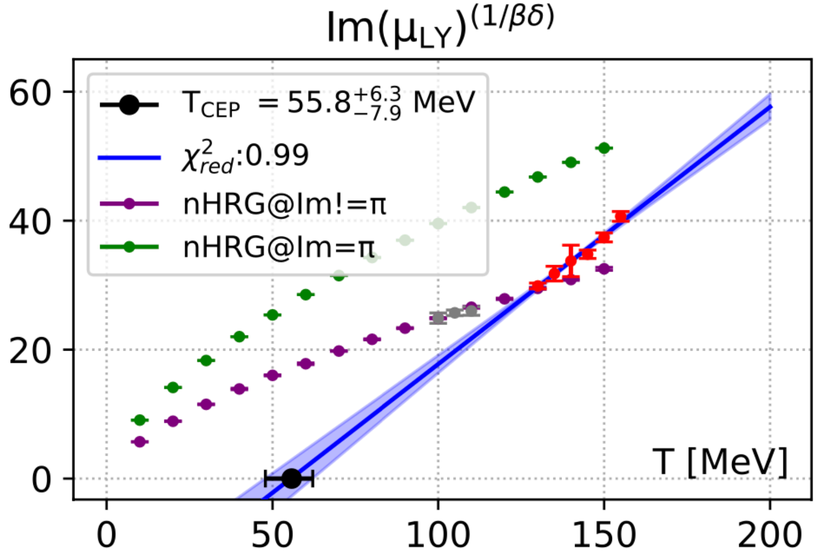


$T^{\mathrm{CEP}} = 105^{+8}_{-18}$ MeV

$\mu_B^{\mathrm{CEP}} = 422^{+80}_{-35}$ MeV

Bielefeld-Parma, arXiv:2405.10196

Lee-Yang edge singularity

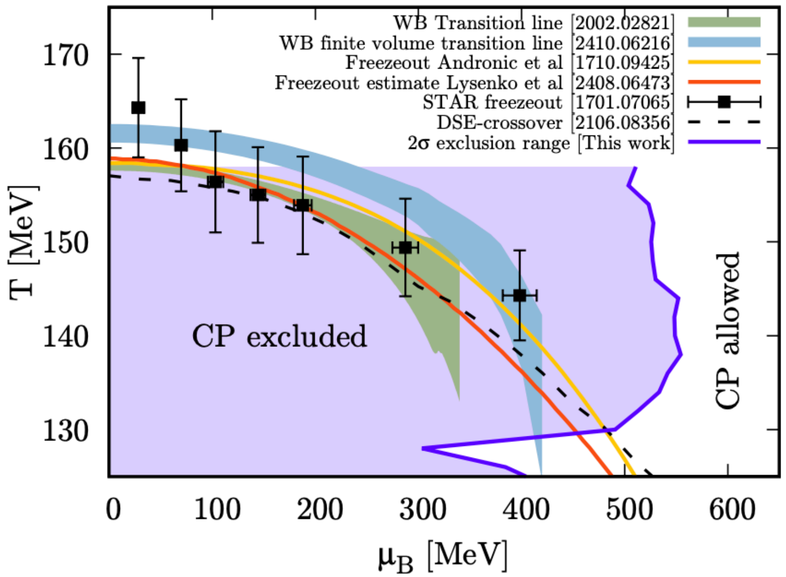


$T^{\mathrm{CEP}} < 103$ MeV
with 84% probability or
CEP does not exit

Adam et al., arXiv:2507.13254

Recent results on the CEP search in Lattice QCD

Contour of constant entropy



No CEP at $\mu_B < 450$ MeV at the 2σ level

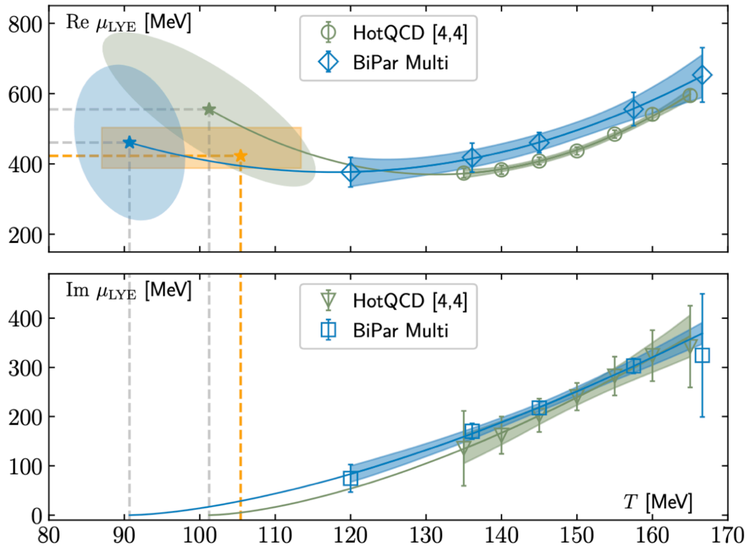
Borsányi et al., arXiv:2502.10267

$T^{\rm CEP} = 114.3 \pm 6.9$ MeV

$\mu_B^{\rm CEP} = 602.1 \pm 62.1$ MeV

Shah

Lee-Yang edge singularity

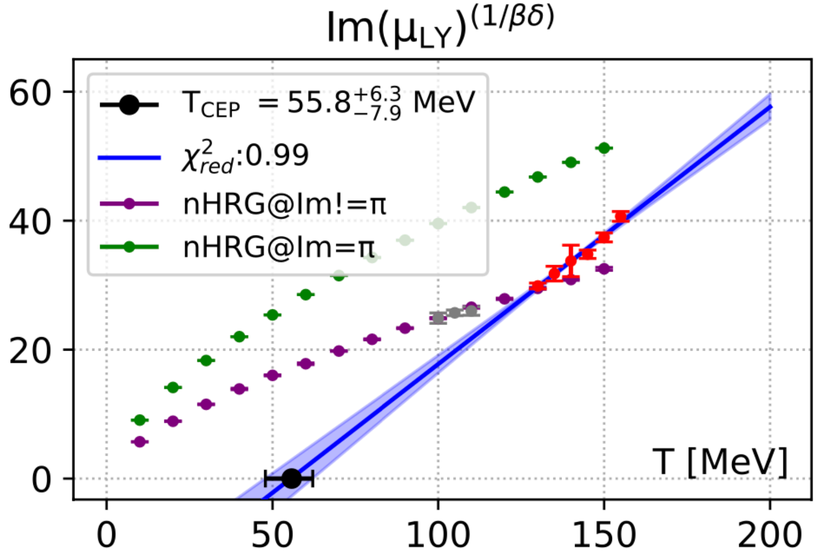


$T^{\rm CEP} = 105^{+8}_{-18}$ MeV

$\mu_B^{\rm CEP} = 422^{+80}_{-35}$ MeV

Bielefeld-Parma, arXiv:2405.10196

Lee-Yang edge singularity



$T^{\rm CEP} < 103$ MeV
with 84% probability or
CEP does not exit

Adam et al., arXiv:2507.13254

All these analyses are done based on extrapolations
from lattice QCD results at $T \gtrsim 120 - 130$ MeV